



**National
Oceanography Centre**
NATURAL ENVIRONMENT RESEARCH COUNCIL

National Oceanography Centre

Internal Document No. 15

How does coastal bathymetry impact
tidal ellipse geometry?

M C Prosser & J M Brown

2015

National Oceanography Centre, Liverpool
6 Brownlow Street
Liverpool
L3 5DA
UK

Author contact details
Tel: 0151 795 4800
Email: mpross@noc.ac.uk
jebro@noc.ac.uk

© National Oceanography Centre, 2015

DOCUMENT DATA SHEET

AUTHOR PROSSER, M C & BROWN, J M	PUBLICATION DATE 2015
TITLE How does coastal bathymetry impact tidal ellipse geometry?	
REFERENCE Southampton, UK: National Oceanography Centre, Southampton, 56pp. (National Oceanography Centre Internal Document, No. 15) (Unpublished manuscript)	
ABSTRACT <p>In this study, the extent to which different bathymetries, imposed in the Liverpool Bay POLCOMS model domain, affect the accuracy of the model output is investigated. In total 4 model simulations with 4 different bathymetries are used. The model velocities are analysed to create (M_2) tidal ellipses where there are observations (both across Liverpool Bay and vertically at 4 locations). Error metrics (<i>RMSE</i>, <i>Bias</i> and <i>Model Skill</i>) are applied to the major axis, minor axis, phase and rotational direction of the ellipses to enable a quantitative comparison between the model and observational data.</p> <p>While the bathymetry from the latest lidar survey (AccBath) is found to have the best match with the observational ellipses the earlier bathymetry is found to do similarly well. These bathymetries are found to enhance the model's predictive ability substantially relative to the 5 and 10 m minimum depth simulations.</p> <p>A comparison of tidal ellipses before and after the installation of the RHYL windfarm site is also carried out but little difference is observed in the M_2 tidal ellipses.</p>	
KEYWORDS	
ISSUING ORGANISATION National Oceanography Centre University of Southampton Waterfront Campus European Way Southampton SO14 3ZH UK	

Page intentionally left blank

1. Introduction.

Liverpool Bay is a shallow and hypertidal (range > 10 m) region of fresh water influence (ROFI) within the eastern Irish Sea. The main inflowing estuaries include the Mersey, the Dee and the Ribble. For further detail of the area see Polton *et al.* (2011).

The Proudman Oceanographic Coastal Ocean Modelling System (POLCOMS) has been used in a number of contexts to model the dynamics in Liverpool Bay and the model output parameters in this domain have been validated in numerous different ways (see Amoudry, 2014; Brown *et al.*, 2015). Traditionally the coastal bathymetry used in the model is the ‘best setup’ bathymetry (The Control simulation in this project), which is a composition of a lidar surveys, between 1999-2010 (See Fig. 1). We wanted to know whether replacing the coastal bathymetry with a more consistent, recent (2010) lidar survey (hereafter referred to as AccBath) led to an improved match between the POLCOMS model generated and the observed (HF radar and ADCP) M_2 tidal ellipses. The M_2 tidal constituent was chosen as it is the largest and accounts for the majority of the tidal motion within Liverpool Bay (Polton *et al.*, 2011).

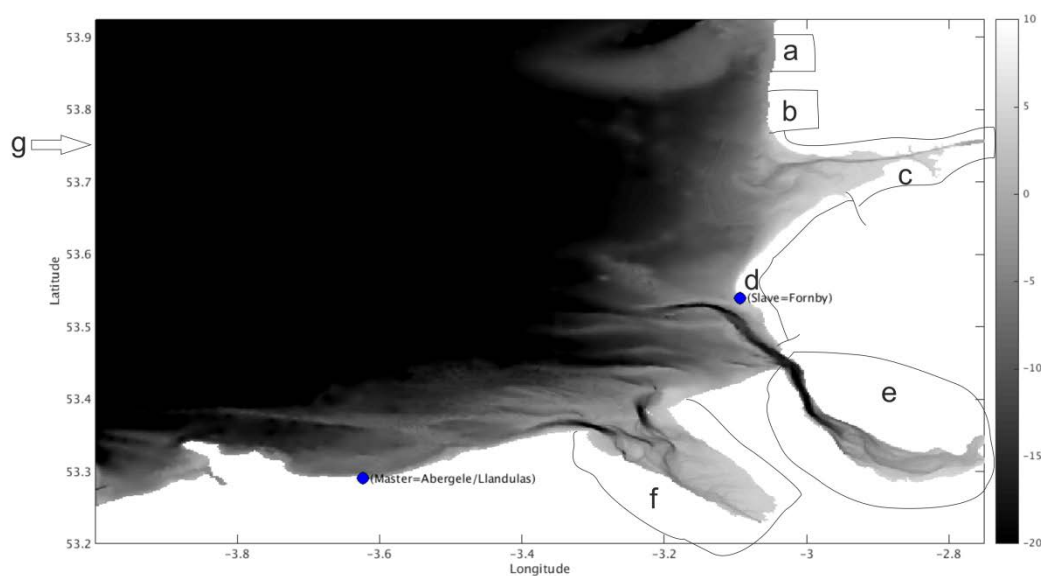


Figure 1: A schematic to show the origins of the ‘Control’ Bathymetry. (a) Fleetwood via Sefton lidar data, February – November 2010. (b) Blackpool via Sefton lidar data, February – November 2010. (c) Ribble via Sefton lidar data, June 1999. (d) Sefton coast Fleetwood via Sefton lidar data, February – November 2010. (e) Mersey estuary via the Mersey Docks & Harbour Company, September 2002. (f) Dee estuary via the EA website, October 2003, June 2004, October 2006 and October 2007. (g) Offshore bathymetry taken from admiralty charts.

The model was run for the representative year of 2008 (see section 1.1) as this has been shown to be typical of the annual metrological and coastal ocean conditions experienced within this region (Norman *et al.*, 2014b). In the end only the first 8 months of the POLCOMS 2008 output were used as the model developed instabilities at the beginning of September when the latest bathymetry (AccBath model simulation) of 2010 was imposed. This was due to small areas (pools) with steep gradients at the estuary margins causing numerical error within the wetting and drying algorithm.

In addition to these 2 bathymetries a 5 m and a 10 m minimum depth simulation were also included to give a sense of how important coastal bathymetry is. Minimum depth simulations are those in

which the bathymetry above 5 or 10 m below MTL is removed (resulting in a flattening of banks around the coast and in estuaries). As a consequence of the 'missing' banks a greater volume of water will flow into and out of the estuaries relative to bathymetries with the channel-bank system included. If the 2010 bathymetric data is found to produce tidal ellipses that align better with the observations than the earlier bathymetry then the significance of this improvement can be evaluated based on the improvement of the earlier bathymetries relative to the 5 and 10 m minimum depth simulations.

Our hypothesis is that: either the model simulation with the 2010 lidar survey bathymetry (AccBath) or the simulation with the control bathymetry (Control) imposed will produce the M_2 tidal ellipses with the best match to the observation derived M_2 tidal ellipses. While the AccBath bathymetry is more recent, the model will be simulating the year 2008 and compared with observations from the period 2006-2008. We hypothesise that the Control and AccBath bathymetries will give a better match between the model and the observation than the minimum depth bathymetries (MinDepth5 MinDepth10).

In addition to the main aim of testing different bathymetries in the model, a further aim was to investigate the degree to which the installation of the RHYL windfarm (Installed between 2007 and December 2009) resulted in a change in the M_2 tidal ellipses.

1.1 The POLCOMS Model Application

In order to investigate the effects different coastal bathymetry have on tidal currents, the 3D Proudman Oceanographic Coastal Ocean Modelling System (POLCOMS) was applied to Liverpool Bay with a resolution of 180 m in the horizontal and 20 levels within the water column in the vertical. The Liverpool Bay domain is nested inside an Irish Sea model, which has a 1.8 km resolution and 32 vertical levels in the water column. The number of vertical levels in the Liverpool Bay is fewer than in the Irish Sea setup, which has a minimum depth of 5 m in Liverpool Bay. This is to minimize the possibility of errors occurring in very shallow locations due to the vertical resolution becoming less than the bed roughness, 0.003 m at low tide. For further detail of the numerical setup, see Holt and James (2001) and the POLCOMS user guide (Holt, 2007).

POLCOMS uses terrain following sigma coordinates in the vertical and incorporates:

1. Bathymetry files from hydrographic and LiDAR surveys,
2. Meteorological data from the UK Met Office numerical weather predictions (Wind, pressure, cloud cover, humidity and air temperature),
3. Data from the National Oceanography Centre's Coastal Observatory pre-operational modelling system to provide large scale circulation, temperature and salinity fields. These are

used as boundary conditions for the Irish Sea model and initial conditions for both the Irish Sea and Liverpool Bay simulations.

4. Daily mean river flow data from the UK national river flow archive at locations where weighting factors to account for the downstream catchment contribution from the gauging station is available (Marsh and Sanderson, 2003).

The model is baroclinic and incorporates algorithms to simulate the wetting and drying of intertidal banks in the shallow regions. In this investigation the model has been run for the year 2008 (up until the end of August) following a model spin up period for the month of December 2007. Data are output from the model every 30 minutes at the locations of interest. Each 8 month simulation for Liverpool Bay took around 5 days using 128 processors of the local NOC cluster (Mobius). The model has been validated at 2 offshore moorings in Liverpool Bay and at the Mersey's Gladstone Dock tide gauge. It has been found to perform well during the year 2008 (see Norman *et al.*, 2014a; Prosser *et al.*, 2014 for further details).

To allow a realistic simulation of annual conditions to provide the Control scenario to assess different coastal bathymetries, the year 2008 was chosen to represent the typical current dominant, wave dominant and wave-current conditions that can occur within the bay for the study of sediment transport (Amoudry *et al.*, 2014; Ramirez-Mendoza *et al.*, 2014; Norman *et al.*, 2014b). Norman *et al.* (2014b) have compared 2008 with long-term data sets of Metocean parameters finding this is a typical year. Here, we have continued to use the same realistic forcing (as in Norman *et al.*, 2014a) to repeat simulations of this year (up until the end of August) under different coastal bathymetric conditions. The full eight months were simulated to enable a suitably long data set to be used in the tidal analysis. In order to investigate the effect of different bathymetries on tidal circulation, all other parameters have been maintained for this representative year.

1.2. Observational Data

1.2.1. ADCP data

In order to investigate tidal ellipses within the water column ADCP data from 4 different sites were used (see Fig. 2). These locations represent all mooring sites where ADCP data were available from the Liverpool Bay Coastal Observatory. Of the four sites, one is located inside the Dee Estuary (Site Hilbre), one is located near the mouth of the Mersey Estuary (Site A) and two are located further offshore (Site B and Site 12). This variation in ADCP site proximity to the coast will enable the influence of shallow coastal bathymetry with distance offshore to be observed. Table 1 details the time series available from each of the 4 sites.

Table 1: Time-series of the 4 sites.

ADCP Site	Start date (Matlab time)	Time interval	End date (Matlab time)
A	(2008,1,1,0,0,0)	half hourly	(2008,12,31,23,30,00)
B	(2008,1,1,0,0,0)	half hourly	(2008,12,31,23,30,00)
Hilbre	(2008,2,14,13,0,0)	hourly	(2008,3,9,10,0,0,0)
12	(2008,2,12,8,9,59.5)	hourly	(2008,3,23,3,10,4.35)

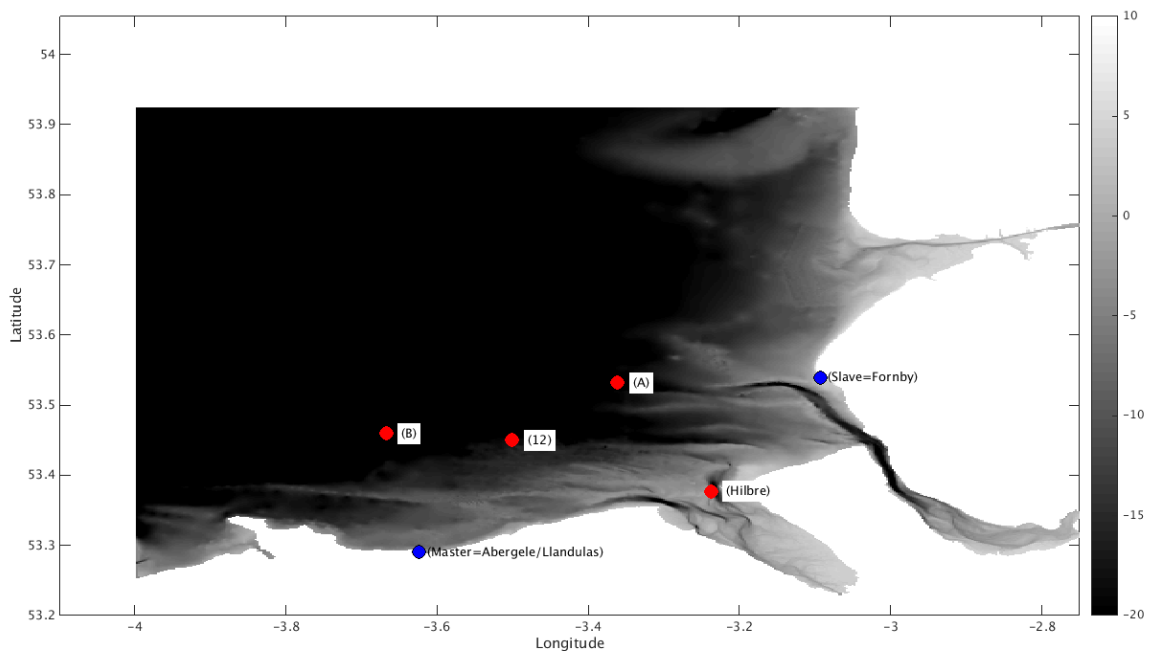


Figure 2: The locations of mooring stations with observations available to investigate the depth-variation in tidal ellipses.

1.2.1. HF radar data

In order to investigate the horizontal variation in surface ellipses data from the Coastal Observatory Liverpool Bay (CObs) program¹ was downloaded. The CObs programs ran from the 1st of August 2005 to the 6th of December 2011 and utilised 2 HF radar sites (One at Abergele and one at Formby; see red circles; Fig. 3) to record u and v velocities across Liverpool bay at 20 minute intervals.

¹ Downloaded from <http://cobs.pol.ac.uk/wera/>

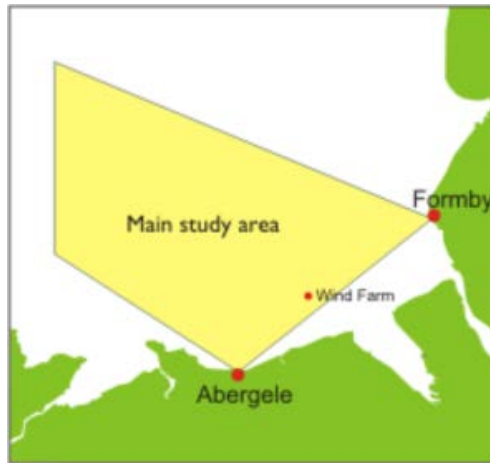


Figure 3: The area of Liverpool Bay over which surface u and v current data was available from the CObs program.

Within the main study area shown in Figure 3, a total of 157 radar cells were available throughout the 2005-2011 period (for locations and number reference of cells, see thick red crosses in Fig. 4). As not all of these cells were active throughout the entire period, data from the period [2006,1,1,0,4,26] to [2006,8,31,4,4,26] was chosen as this maximised the number of cells that were active (108 out of the 157 cells).

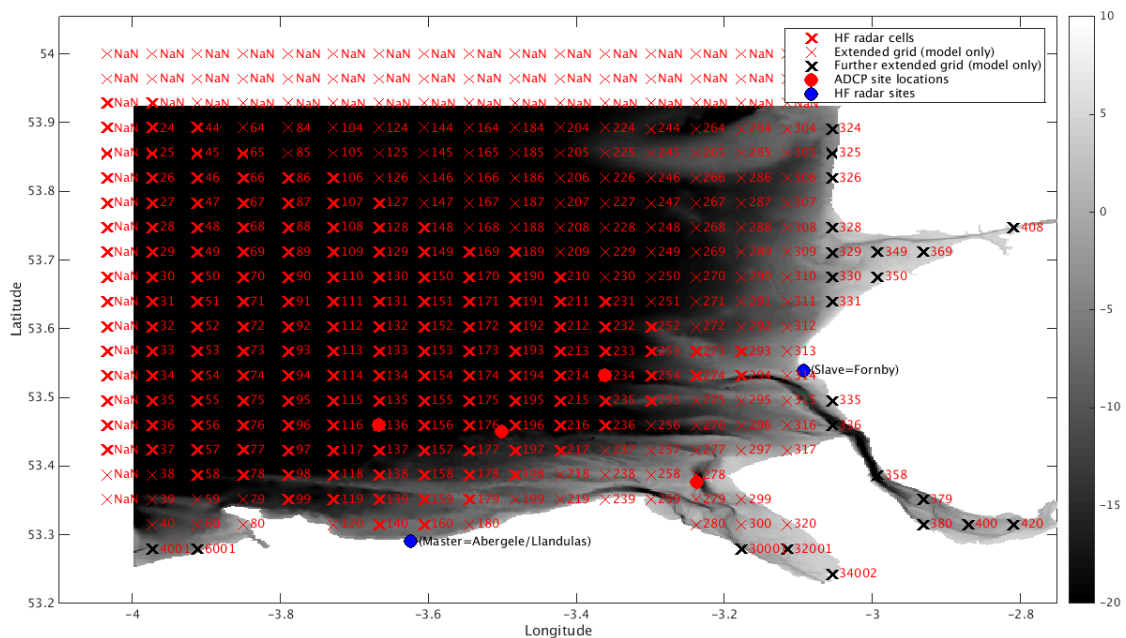


Figure 4: The thick red crosses denote the HF radar cells where surface u and v are recorded. The thin red crosses and the thick black crosses are where only model u and v data is available. HF radar data outside of the Liverpool domain has been ignored in this analysis (set to NaN in Fig. 4). Each cell has a reference number as in the figure.

1.3. Tidal ellipses

In order to compare the modelled and observed u & v velocity components in a meaningful way, the velocities were represented as tidal ellipses. Tidal ellipses give a visual indication of the average tidal flow over a certain time period. The major axis indicates the main direction of tidal flow while the minor axis is (among other things) a result of the Coriolis force acting on the flow as it moves backward and forwards (see Fig. 5). In areas where the tidal flow is constrained by bathymetry (such as in estuarine channels) the flow will tend to be more rectilinear. Tidal ellipses will often (although not always) rotate clockwise in the northern hemisphere. For further discussions on tidal ellipses see Polton *et al.* (2011) and Prandle (1982).

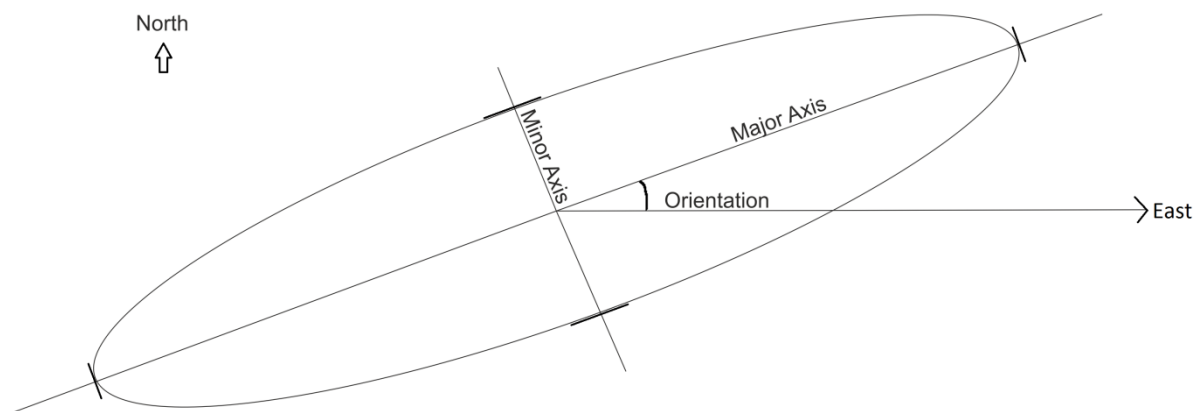


Figure 5: A tidal ellipse showing the major and minor ellipse and the orientation (degrees anticlockwise from due east).

Prandle *et al.* (2011) make 3 comments about M_2 tidal ellipses in coastal regions, which may be relevant here. These comments will be revisited at the end of this report.

1. Tidal currents vary only gradually offshore but vary much more rapidly in shallow water once they pass the 10 m bathymetry contour.
2. In the regions closest to the shore, the major axes of the tidal ellipses tend to be directed more shoreward.
3. The vertical structure of the clockwise rotating currents is greater than that of the anticlockwise resulting in surface current ellipses tending to rotate clockwise and near-bed ellipses tending to rotate anticlockwise.

1.4. Error metrics

In order to quantitatively compare model ellipses with observations derived ellipses, 3 error metrics were applied to the major axis, minor axis, ellipse orientation and rotational direction of the ellipses.

The first error metric was the Root Mean Square Error (*RMSE*)

The *RMSE* is calculated using the formula below:

$$RMSE = \sqrt{(M - O)^2} \quad (3)$$

A smaller value indicates better model performance.

The *Bias*:

$$Bias\ of\ the\ mean = \bar{M} - \bar{O} \quad (4)$$

Where *M* represents the model values and *O* represents the observed values. The mean, depicted by the over bar, of each is calculated using the following formula:

$$\bar{X} = \frac{1}{n} \sum_{k=1}^n X_k \quad (5)$$

With *n* signifying the total number of data points.

The *Bias* gives a sense of whether the model over or under predicts. A value of 0 suggests an unbiased estimator.

The Willmot (1981) *Model Skill* score, *D*, gives a value of 1 for complete agreement between the model estimator and 0 for total disagreement.

$$D = 1 - \frac{\overline{(M-O)^2}}{(|\bar{M}-\bar{O}|+|\bar{O}-\bar{O}|)^2} \quad (6)$$

The *D* formula breaks down if the observations values are constant or show little scatter (e.g. all a single value). In this instance the denominator will equal the numerator resulting in a *D* value of 0 irrespective of how good a match there is between the model and the observations.

2. Method

In order to identify the degree to which accurate coastal bathymetry impacts on the tidal dynamics (ellipse orientation, rotational direction) the following 3 steps were followed.

1. The model was run with the appropriate setup. For the AccBath simulation, the bathymetry had to be prepared².
2. The model output (u and v currents) was then analysed by UTide (Codiga, 2011) to extract the M_2 amplitudes and phases.
3. The M_2 amplitudes and phases were then used to generate and plot tidal ellipses both across Liverpool Bay (HorizEllipse.m³) and with depth at 4 locations (DepthEllipse.m⁴).
4. Error metrics (*RMSE*, *Bias* and *Model Skill (D)*) were then calculated in order to quantify each model simulations match with the observations.

In total 4 simulations were carried out.

Note: Rather than one script calling a function which might then call another function, the following method uses a step-by-step approach whereby a script will be run, outputs will be saved and then loaded into other scripts etc. This approach was chosen as the former can be time inefficient when repeatedly analysis the extracted data.

² Script can be found at /projectsa/intertidal/HFradar/matlab/Liv_bathyMCP/read_POLCOMS_bath_2

³ Script can be found at /projectsa/intertidal/HFradar/matlab/HorizEllipse.m

⁴ Script can be found at /projectsa/intertidal/HFradar/matlab/DepthEllipse.m

Table 2: Model scenarios.

Model simulation	Description
Control	Using the 'best setup' which involved using atmospheric temperature as a proxy for river temperature, includes surface heat flux calculations, sets river salinity to 0 psu but excludes waves in this study for computational efficiency ⁵ . The bathymetry is based on different sources taken between 1999 and 2010 (See Fig. 6) and has the main channel of the Mersey artificially deepened to ensure that river flow is discharged at low water (Prosser <i>et al.</i> , 2015).
MinDepth5	Liverpool Bay and Mersey estuary bathymetry set to a minimum depth of 5 m relative to the MTL at Gladstone Dock removing the shallowest parts of the channel-bank structure.
MinDepth10	Same as above except set to a minimum depth of 10 m.
AccBath	As in 'Control', but with more recent coastal bathymetry (Based on a Lidar Survey in 2010 imposed in the model ⁶).

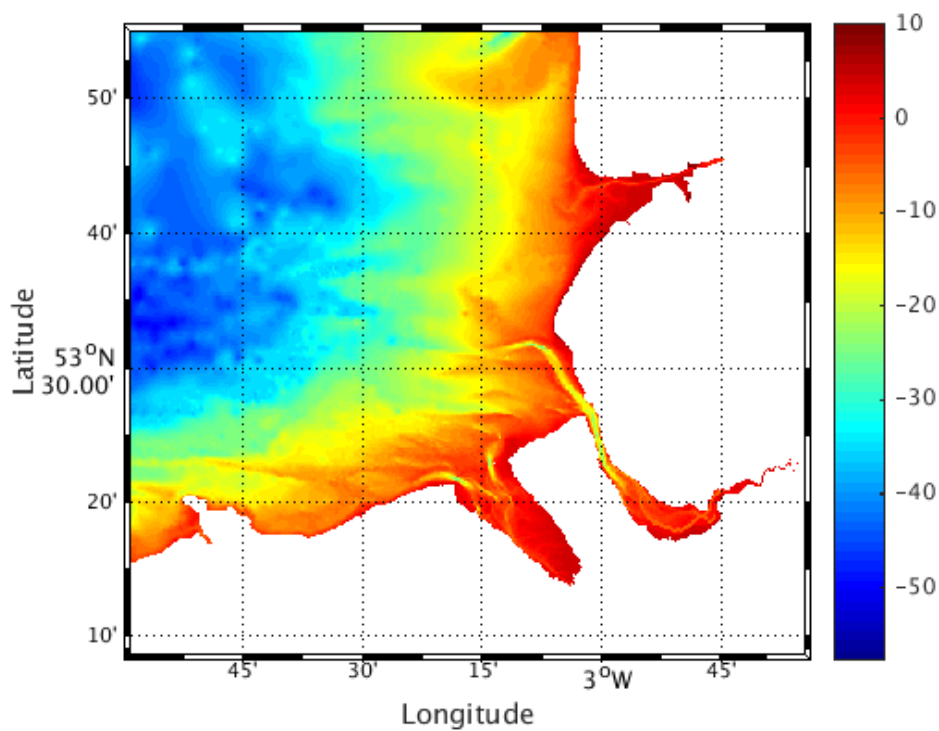


Figure 6: The 'best setup' bathymetry used for the Control simulation, see Table 2.

⁵ Bathymetry input files for the Control simulation can be found at /projectsa/iCoast/Mersey_CEFAS/LB2008/Danielle/LB_rivChannels_bathy_DN.txt

⁶ Script can be found at /projectsa/intertidal/HFradar/Matlab/Liv_bathyMCP/read_POLCOMS_bath_2.m

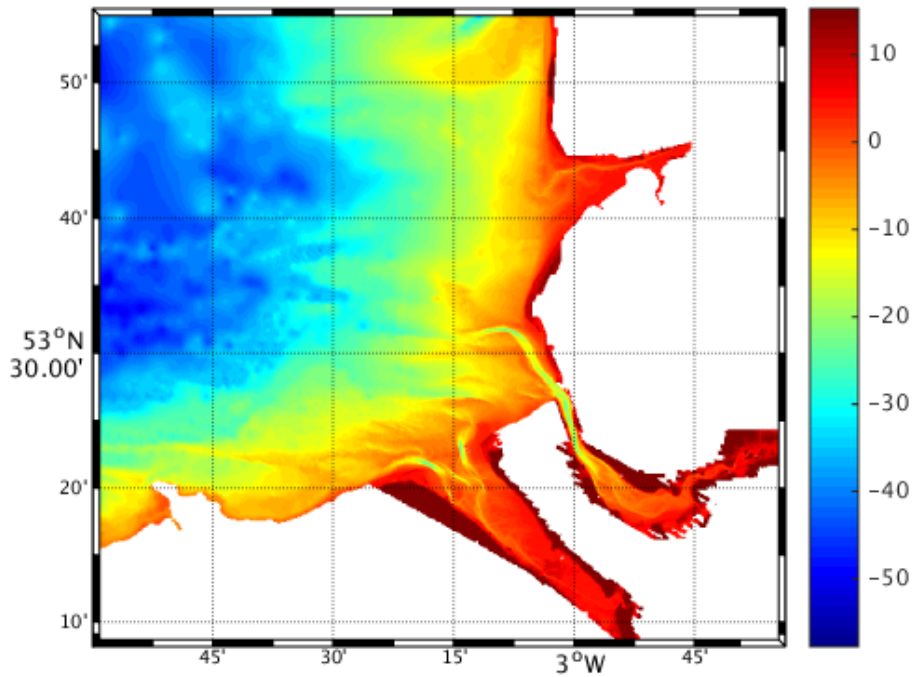


Figure 7: The 'AccBath' bathymetry, see Table 2.

While Figure 7 shows the bathymetry used for the AccBath simulation, the model (due to the way it has been set up) treats any bathymetry that is higher than 10 m above the mean tidal level (MTL) as dry land. Figure 8 therefore gives a better indication of the bathymetry that the model uses in the computational domain.

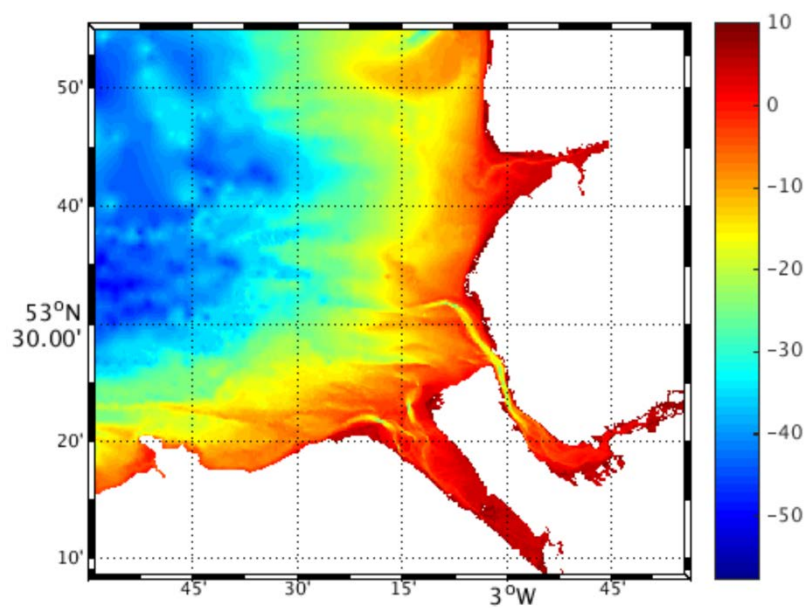


Figure 8: The computational area of the ‘AccBath’ bathymetry as used by this the model setup, see Table 2, with all locations above 10 m above MTL set to dry land.

2.1. Depth-varying ellipses.

2.1.1. Loading in and processing the ADCP observations.

2.1.1.1. Site A and B

The script ADCP_ZUV.m⁷ extracts the site A and B u and v velocity ADCP data (These time-series are for the whole of 2008) and interpolates it in time (to 30 minute intervals to match the model data) and space (onto 20 velocity sigma levels).

The interpolated surface u and v for site A and B were saved⁸ and loaded in at the beginning of the DepthEllipse.m script, which plots the depth varying ellipses from this data.

2.1.1.2. Site Hilbre

The script Hilbre_validationMCPmod.m⁹ was used to import and process the pre-processed Hilbre ADCP data (Bolanos *et al.*, 2010). The data is hourly and covers the time period [2008 2 14 13 0 0] to [2008 3 9 10 0 0]. The first 7 hours are removed as this is the deployment period and the data is interpolated onto the 20 sigma levels to enable comparison with the model. As the Hilbre data sits in a channel (roughly aligned south easterly), the rotmajax.m¹⁰ function was applied to the u and v currents of each sigma level to align them into cross and along channel components to prevent error in channel alignment between the model and observations influencing the error metrics. At this stage the error metrics were calculated. The Hilbre velocity components for all model simulations and observations were then manually rotated back by the depth mean value that the Hilbre observations were initially rotated by. This was to allow visual comparison with the other 3 sites plotted in Cartesian (north east) co-ordinates in Figures 10-13. The final u and v current variable for Hilbre (Uint, Vint) were then saved¹¹ and were loaded in at the beginning of the DepthEllipse.m script to create Figures 10-15.

2.1.1.3. Site 12

⁷ Script can be found at /projectsa/intertidal/HFradar/Matlab/ADCP/ADCP_ZUV.m

⁸ Saved at /projectsa/intertidal/HFradar/Matlab/Loaded_in_by_other_scripts/DepthStartVar08jan.mat

⁹ Script can be found at /projectsa/intertidal/HFradar/Matlab/Hilbre/Hilbre_validationMCPmod

¹⁰ Script can be found at /projectsa/intertidal/HFradar/Matlab/Hilbre/rotmajax.m

¹¹ Saved at /projectsa/intertidal/HFradar/Matlab/Hilbre_validationMCPmodFV/RotRotBack22may.mat;

The script Site12script.m¹² was used to import and process the Site 12 ADCP data¹³ (See Bolaños and Souza, 2010). The data is hourly, and covers the time period [2008 2 12 8 9 59.5] to [2008 3 23 3 1 44]. The data is interpolated onto the 20 sigma levels to enable comparison with the model.

The u and v currents (Uint12, Vint12) were saved¹⁴ and loaded in at the beginning of the DepthEllipse.m script.

2.1.2. Loading in the model data.

Because u and v are vector variables, POLCOMS outputs these at discrete points centred on the grid cells. As the geographical coordinates of the 4 sites were unlikely to coincide exactly with the centre of the model grid cells, the which4of16.m¹⁵ script was used to extract a time series of u and v at the 4 nearest grid cells to each of the 4 locations. The ValidationUVvalues.m¹⁶ script was then used to separately compare the model u and v values of the nearest 4 grid cells with the ADCP observations at that location using equation 1.

$$\begin{aligned} & (\sum_{i=1}^{*total} (\text{ObsU}_{**top} - \text{ModelU}_{top})^2 + \sum_{i=1}^{total} (\text{ObsV}_{top} - \text{ObsV}_{top})^2)^{0.5} + \\ & (\sum_{i=1}^{total} (\text{ObsU}_{**mid} - \text{ModelU}_{mid})^2 + \sum_{i=1}^{total} (\text{ObsV}_{mid} - \text{ObsV}_{mid})^2)^{0.5} + \\ & (\sum_{i=1}^{total} (\text{ObsU}_{**bottom} - \text{ModelU}_{bottom})^2 + \sum_{i=1}^{total} (\text{ObsV}_{bottom} - \text{ObsV}_{bottom})^2)^{0.5} \end{aligned} \quad (1)$$

*total refers to the total number of model outputs for the Control simulation in the year 2008 that could be compared with observations.

**top/mid/bottom refers to u and v taken at different depths of the water columns.

The grid cell with the lowest error (from Eq. 1) was selected as the grid cell point to be used when comparing the tidal ellipses from the model with the tidal ellipses from the observations.

¹² Script can be found at /projectsa/intertidal/HFradar/Matlab/Site12/Site12script.m

¹³ The raw data can be found at /projectsa/intertidal/HFradar/Matlab/Site12/Site12script.mat.

¹⁴ Saved at /projectsa/intertidal/HFradar/Matlab/Loaded_in_by_other_scripts/Interp20site12

¹⁵ Script can be found at /projectsa/intertidal/HFradar/Matlab/Which4of16.m

¹⁶ Script can be found at /projectsa/intertidal/HFradar/Matlab/ValidationUVvalues.m

Table 3: ADCP and corresponding POLCOMS cell coordinate

Location	ADCP coordinates	Cell coordinate (Cell number/Relative Position to ADCP)
Site B	-3.6674 / 53.4597	-3.6638 / 53.4592 (3/SE)
Site 12	-3.500556 / 53.45	-3.5012 / 53.4508 (5/NW)
Site A	-3.3611 / 53.5317	-3.3587 / 53.5342 (12/NE)
Site Hilbre	-3.2375 / 53.377222	-3.2337 / 53.3775 (15/NE)

The model u and v time series for the 4 locations (Table 3) were extracted using the which4of16.m script and loaded into the DepthEllipse.m script. Site Hilbre required some extra processing before loading into the DepthEllipse.m script as described in Section 2.1.1.2.

The DepthEllipse.m script then performs the following steps.

1. Initialises an abg matrix ($a = M_2$ ellipse major axis, $b = M_2$ ellipse minor axis and $g = M_2$ phase in radians) for each of the 5 data sets at each of the 4 locations. The values of a and b are multiplied by 0.1 in order to scale down the size of the eventual ellipses for visualisation.
2. Applies UTide¹⁷ to each of the 20 data sets (4 model simulations and 1 set of ADCP data for each of the 4 locations), to extract the M_2 ellipse major axis (a), M_2 ellipse minor axis (b) and M_2 phase (g). These values are then stored in the respective abg Matrix.
3. A second matrix (with 64 rows and 6 columns) generically called *EllipseMat* is created for each tidal ellipse of each of the 20 data sets. This matrix stores the coordinate location (64 rows) with the following information for plotting purposes:
 - Column1: Contains $a * \cos \Theta$ (Θ varying from 0 to 2π in $1/64^{\text{th}}$ increments).
 - Column2: Contains $b * \sin \Theta$ (Θ varying from 0 to 2π in $1/64^{\text{th}}$ increments).
 - Column3: Contains the result of the previous 2 columns in the form of a complex conjugate ($z_1 = \text{Column1} + \text{Column2} * i$)
 - Column 4: performs the following operation on column 3.
$$z_2 = z_1 * e^{i * g} \quad (2)$$
 - Column 5: the x-coordinate is the real part of the complex conjugate z_2 and is added to the longitudinal coordinate for the respective location so as to centre the ellipse on that location (e.g. -3.3611 west for site A).
 - Column 6: the y-coordinate is the complex part of the complex conjugate z_2 and is added to the depth of that ellipse (centring on the 20 velocity sigma depth levels in the model (-1 being the bed and 0 being the surface) for visualisation in Figs. 10-15.

¹⁷ As Utide can deal with gaps in tidal time-series, it was chosen over T-tide to perform the tidal analysis in this project.

4. For each ellipse DepthEllipse.m then calculates whether the ellipse is rotating clockwise or anticlockwise. If the minor axis has a positive value the rotation is anticlockwise, if it has a negative value the rotation is clockwise.
5. The ellipses are then plotted (see Figs. 10-15).

2.2 Horizontal-variation in surface ellipses.

2.2.1. Loading in the model data.

In order to load and process the model data across the HF radar model grid the following scripts were used in the following order.

ZetUSVS.m¹⁸ -> ProcessModelData.m¹⁹ -> HorizEllipse.m.

ZetUSVS.m extracts 2x 3D matrices for each month (of the u and v velocities). Each matrix has size $576 \times 474 \times (\text{number of hours for that month})$. Before UTide can be applied, the model data needs to be interpolated onto the HF radar coordinates. This is done using the ProcessModelData.m script.

ProcessModelData.m loads in the 3D matrices and proceeds to format it for comparison with the observations. The matrices are rotated by 90 degrees anticlockwise before performing 'flipud' on the matrices. Each time step (hourly) the u and v values are then interpolated onto the coordinates of the HF radar cells and 2 new 2D matrices (Name format: NAMEOFMODELRUNHEREInterpU, NAMEOFMODELRUNHEREInterpV) are generated with 334 columns (number of HF radar cells plus extras) and 744 rows (or the number of hours for that particular month).

These 2 matrices are then loaded in at the beginning of the HorizEllipse.m script.

HorizEllipse.m first initialises an abg matrix (The M_2 major tidal axis (a), minor tidal axis (b) and orientation (g) see section 2.1.2) for every location (334) of each model run before applying UTide to each column of each model simulations' InterpU and InterpV.

The UTide algorithm is of the following form:

UTide output Structure = ut_solv(date vector, InterpU matrix, InterpV matrix, latitude VARARGIN.....)

Utide outputs the a b and g into the corresponding abg matrix and from these matrices a corresponding 6 column *Ellipse Matrix* is generated²⁰. The ellipses from either one or multiple model simulations can then be plotted over the Liverpool Bay domain (see Figs. 16-23).

2.2.2. Loading in the HF radar observations.

The HorizEllipse.m script then calls the plot_ellipses.m²¹ script to plot the HF radar derived M_2 tidal ellipses alongside the modelled ellipses.

¹⁸ Script can be found at /projectsa/intertidal/HFradar/Matlab/ZetUSVS.m

¹⁹ Script can be found at /projectsa/intertidal/HFradar/Matlab/whywhy.m

²⁰ See section: Ellipses with depth: Loading in the model data: Step 3 for procedural details.

The plot_ellipse.m script calls the extract_currents.m function to load in the HF radar observations.

The extract_currents.m script loads in the raw data²², which is in 4 columns:

Column 1: Time in seconds since [1970 1 1 0 0 0].

Column 2: Wind direction (degrees clockwise from north).

Column 3: Current direction (degrees clockwise from north).

Column 4: Current speed (m/s).

Then 266 seconds is added to the time column. Data collection takes 532 seconds in total so 266 seconds is added to the time column to get the correct mid time of the collected data. As the raw BODC data has gaps where data has not been recorded, extract_currents.m uses a loop to include the missing dates so that the time series is continuous. The time column is then converted into a Matlab number (datenum).

Finally the data is quality controlled. This is done by eliminating any current values higher than 1.5 m/s and then by replacing the original current values with a 3 data point moving average²³ of the currents.

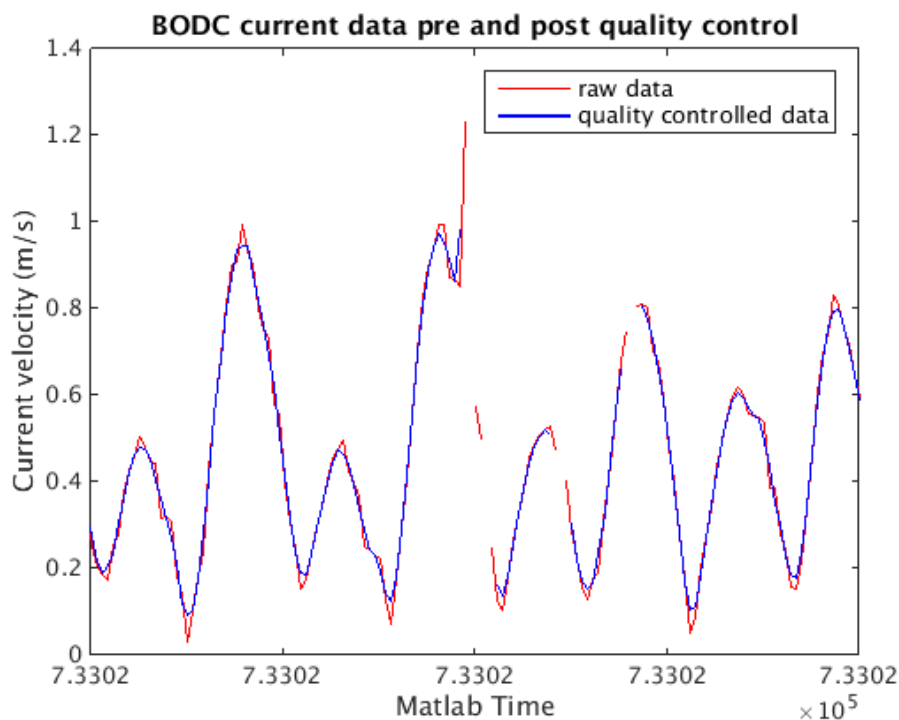


Figure 9: An example of what the data looks like pre and post the extract_current.m quality control process.

²¹ Script can be found at /projectsa/intertidal/HFradar/Matlab/plot_ellipses.m

²² Raw data downloaded from the BODC website: <http://cobs.pol.ac.uk/wera/>

²³ This function was downloaded from <http://www.mathworks.com/matlabcentral/fileexchange/8251-moving-averages---moving-median-etc> Site last accessed 17/04/2015.

The plot_ellipses.m script then proceeds to process the data provided by the extract_currents.m script. First, the u and v current velocities are derived from the magnitude and direction of the current data using trigonometry. As the 157 HF radar cells do not all have data over 2008, the data for the period [2006,1,1,0,4,26] to [2006,8,31,44,26] was chosen as the nearest complete data set. The script LengthTime.m²⁴ was used to identify this period as that when the greatest number of cells had data. Utide was applied to the data in order to generate *ellipse* matrices²⁵. Plot_ellipses.m then plotted the observations on top of the modelled ellipses previously plotted by HorizEllipse.m (using an ellipse plotting function called plot_ellipse.m²⁶).

2.3. Method: Tidal Ellipses pre and post wind farm.

In order to plot the tidal ellipses before and after the wind farm installation the plot_ellipses.m script was run twice, once to plot the ellipses before the installation (period [2007 12 1 0 4 26] to [2008 11 30 23 44 26]) and after the installation (period [2010 12 1 0 4 26] to [2011 11 30 23 44 26]). These time periods were chosen because they enable the maximum number of HF radar cells to be used (108 out of a total of 157 cells).

NB some modifications are required to the plot_ellipses.m script to enable it to plot the before and after wind turbine installation ellipses (see comments in the plot_ellipse.m script for further details). Its default setup enables it to work when called by the HorizEllipse.m script and not automatically for other purposes.

2.4. Calculating the error metrics

While the performance of POLCOMS under different bathymetric scenarios can be evaluated qualitatively by viewing the model generated M_2 tidal ellipses superimposed onto observation generated tidal ellipses, a more quantitative evaluation is desirable. To this end scripts to calculate the *RMSE*, *Bias* and *Model Skill (D)* for the ellipses varying with depth (ErrorMetricsDNew.m²⁷) and for the surface ellipses (ErrorMetricsHNew.m²⁸) were created. The following discusses how these error metrics were applied to the ellipse parameters in both scripts.

2.4.1. Applying error metrics to the major and minor axis

²⁴ Script can be found at /projectsa/intertidal/HFradar/Matlab/LengthTime.m

²⁵ See section: Ellipses with depth: Loading in the model data: Step 3 for procedural details.

²⁶ This function was downloaded from http://www.mathworks.com/matlabcentral/fileexchange/8604-plot-ellipse/content/plot_ellipse.m last accessed 17/04/2015.

²⁷ Script can be found at /projectsa/intertidal/HFradar/Matlab/ErrorMetricsDNew.m

²⁸ Script can be found at /projectsa/intertidal/HFradar/Matlab/ErrorMetricsHNew.m

The calculation of the *RMSE*, *Bias* and *D* were easily applicable to the major and minor axes of the model ellipses. If the model ellipse's major axis was bigger than the corresponding observational ellipse then a positive *Bias* would result, if smaller, then the *Bias* would be negative. Applying these error metrics to the ellipse orientation and the rotational direction however were not as straightforward and some further processing of the results were required. The following section applies to both the `ErrorMetricsDNew.m` and `ErrorMetricsHNew.m` scripts.

2.4.2. Ellipse orientation & rotational direction

The orientation of an ellipse is defined as the number of degrees anticlockwise between the due east direction and the major axis of that ellipse (See Fig. 5). This leads to the situation where an ellipse with an orientation of 179 degrees, if pushed a further 2 degrees anticlockwise becomes equivalent to an ellipse with an orientation of 1 degree. In order for this periodic nature of the orientation to not cause problems for the error metrics, it was decided that the maximum possible difference in the orientation of 2 ellipses was 90 degrees (i.e., the axis are perpendicular when maximum error occurs). Both the `ErrorMetricsDNew.m` and `ErrorMetricsHNew.m` scripts call a function `Phase.m`²⁹ which uses the acute angle between the major axes of the model and observation ellipse to calculate the relative difference in orientation. This ensures the difference (M-O) is always between ± 90 degrees with an orientation difference of 0 degrees being an exact match. This could then be used to calculate the *RMSE* (Eq. 3). To calculate the difference (M-O) in the *Bias* and the *D* (Eq. 4 & 6), the acute angle between the major axes of the model and observation ellipse was used. A negative *Bias* therefore indicates that the model is tending to predict ellipses that are biased clockwise relative to the observation ellipses whereas a positive *Bias* would mean a general *Bias* anticlockwise relative to the observation ellipses. The acute angle was required in calculating the *D* as the formula (Eq.6) encounters problems if the observations are all the same value (e.g. 0).

The rotational direction of the ellipse was identified by the sign of the minor axis. A negative minor value indicates a clockwise ellipse and a positive minor axis value indicates an anticlockwise ellipse. (NB. Later on in both the error metric scripts the absolute value is used so any negative minor values are changed to positive ones in order for a later part of the scripts which ascertains the ellipse with the largest major axis, minor axis, phase etc to function correctly.) Column 5 of the *abg* matrices contains a '1' and column 6 contains a 'NaN' if the rotation is clockwise and vice-versa if the rotation is anticlockwise. In order to calculate the *RMSE* of the rotational direction the M – O is set to '0' to represent an agreement in rotational direction and '1' to represent disagreement. The *RMSE* across all the model ellipses should therefore be '0' if all rotate in the same direction as the observation ellipses and '1' if they all rotate in the opposite direction. In order to calculate the *Bias* and the *D* of the rotational direction, a value of '1' was input into column 7 of every *abg* matrix if the rotation was clockwise and '0' if the rotation was anticlockwise (based on the values in columns 5 and 6 of the *abg* matrices). This meant that if the model ellipse was rotating clockwise while the observation ellipse was rotating anticlockwise the 'M – O' part of Eq.4 and Eq.6 would be '1', '0' if they were rotating the same way and '-1' if the model ellipse was rotating anticlockwise and the observation ellipse was rotating clockwise. In these circumstances a positive *Bias* would indicate that the model was over-predicting clockwise ellipses while a negative *Bias* would indicate an over-prediction of anticlockwise ellipses in Liverpool Bay.

²⁹ Function can be found at [/projectsa/intertidal/HFradar/Matlab/Phase.m](#)

2.4.3. Plotting the RMSE over Liverpool Bay

In order to visualise the spatial accuracy of the model, a combined *RMSE* was calculated over Liverpool Bay (See later Section 4.2).

The RMSELB³⁰ script averages the index of the major axis *RMSE*, minor axis *RMSE* and orientation *RMSE* to calculate a combined *RMSE* for each surface ellipse. This is done using equation 3.

$$\text{Combined RMSE} = \frac{\text{Major axis RMSE index} + \text{Minor axis RMSE index} + \text{Orientation RMSE index}}{3} \quad (3)$$

With each index in the top line of equation 3 being calculated in a similar manner to the major axis *RMSE* index example in equation 4.

$$\text{Major axis RMSE index} = \frac{\text{Individual surface ellipse major axis RMSE}}{\text{maximum major axis RMSE value across all surface ellipses}} * 100 \quad (4)$$

The output variable is then saved³¹ and loaded in at the beginning of PlotCellInfo.m where it is plotted using the pcolor function in Matlab with interpolated shading.

³⁰ Script can be found at /projectsa/intertidal/HFradar/Matlab/RMSELB.m

³¹ Variable can be found at /projectsa/intertidal/HFradar/Matlab/PlotCellInfoFV/Plural.mat

3. Results

3.1. Results: Depth-varying ellipses.

The following Figures (10-15) show the model performance at the 4 sites. In general the model is found to agree well with the observations. See the error metrics (section 4.1, Tables 4-12) for a quantitative comparison between the model derived and observation derived ellipses.

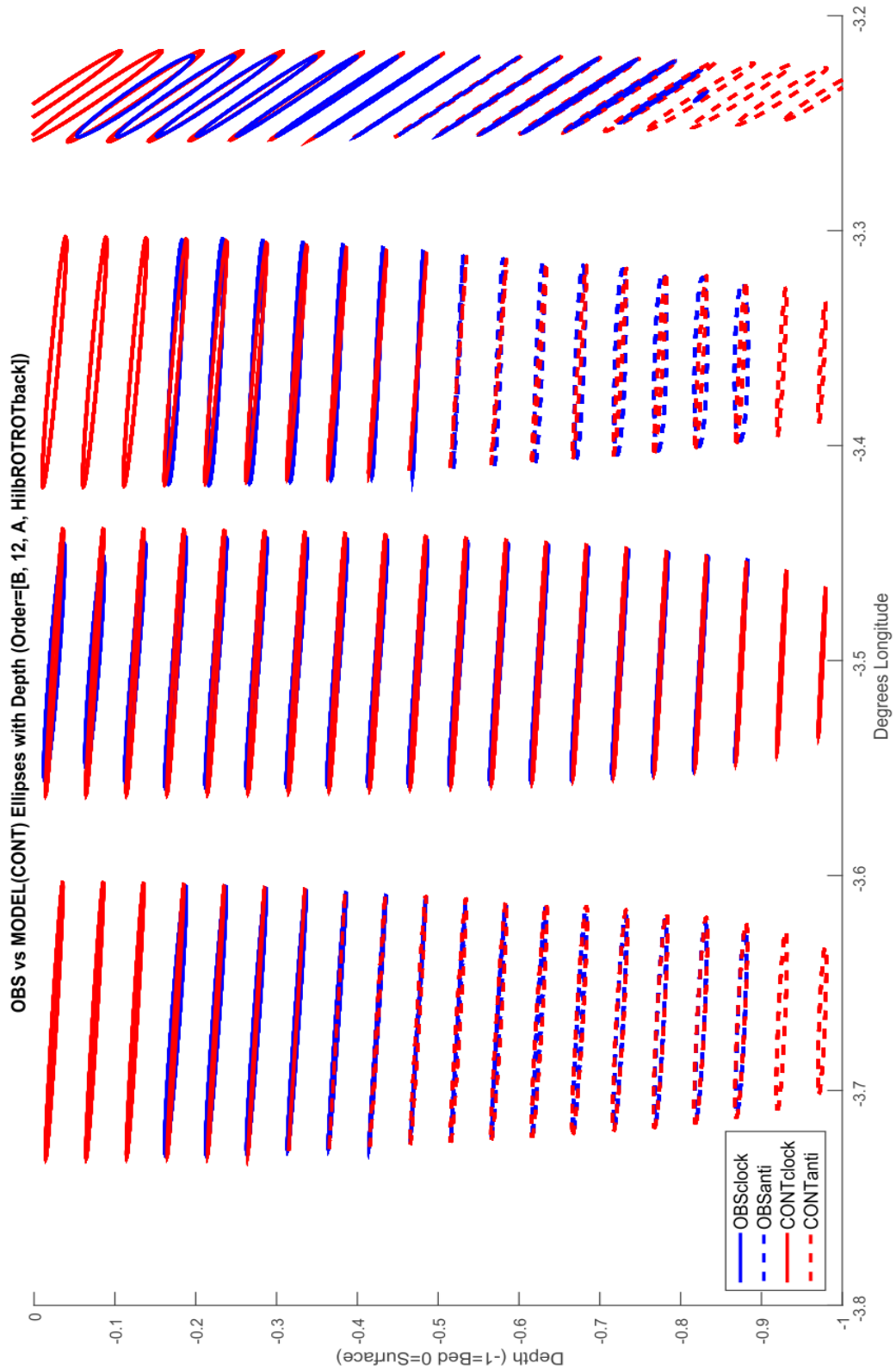


Figure 10: The depth-varying tidal ellipses generated from both the ADCP data and the model output for the 'Control' simulation for the 4 sites. NB although the y-axis indicates depth, each ellipse is seen as if it were a bird's eye view (The major and minor axis of the ellipse representing the north east variability in the tidal ellipse). See Tables 4-12 (Section 4.1) for error metrics relating to depth-varying ellipses.

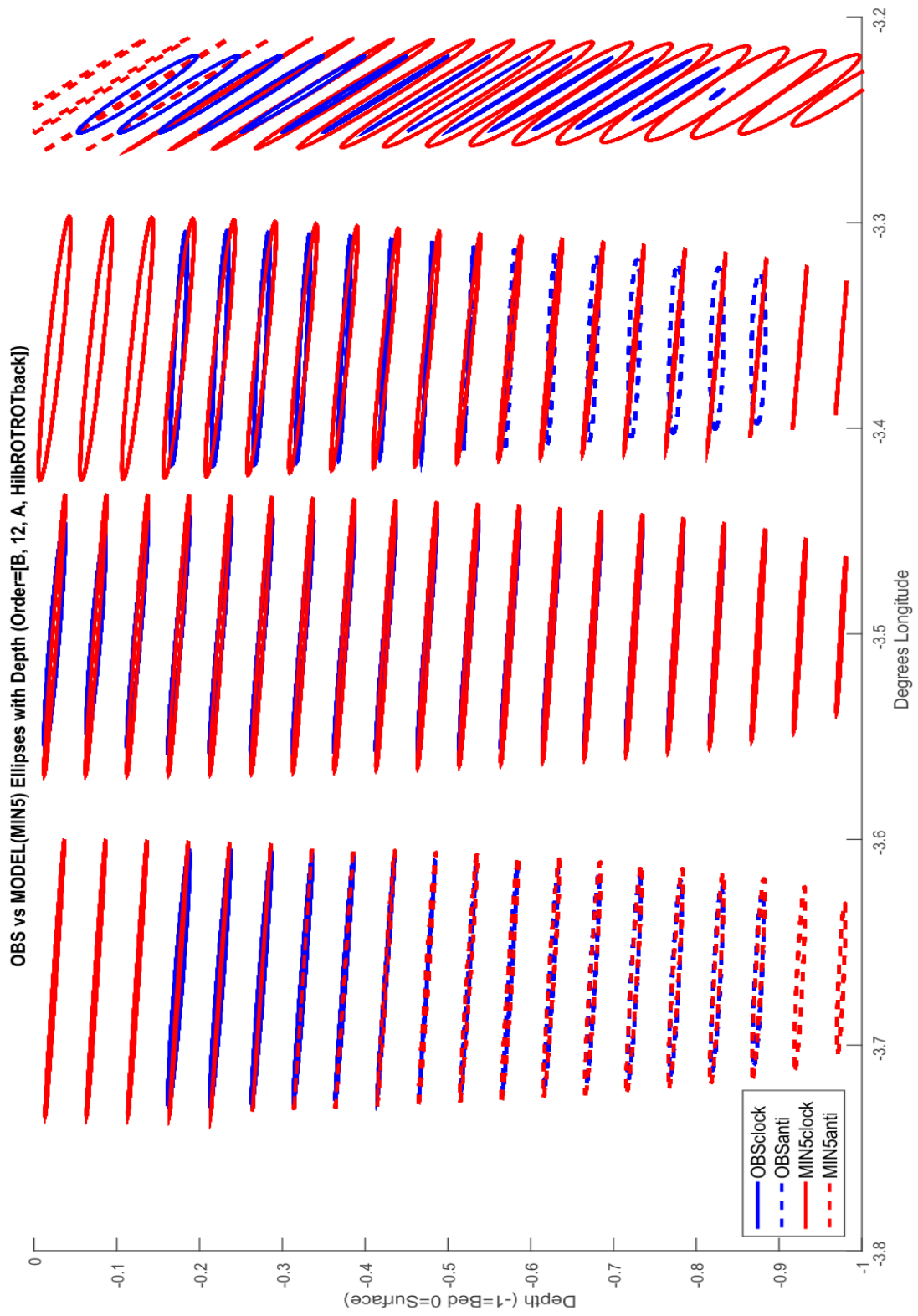


Figure 11: As in Fig. 10, but for the 'MinDepth5' simulation.

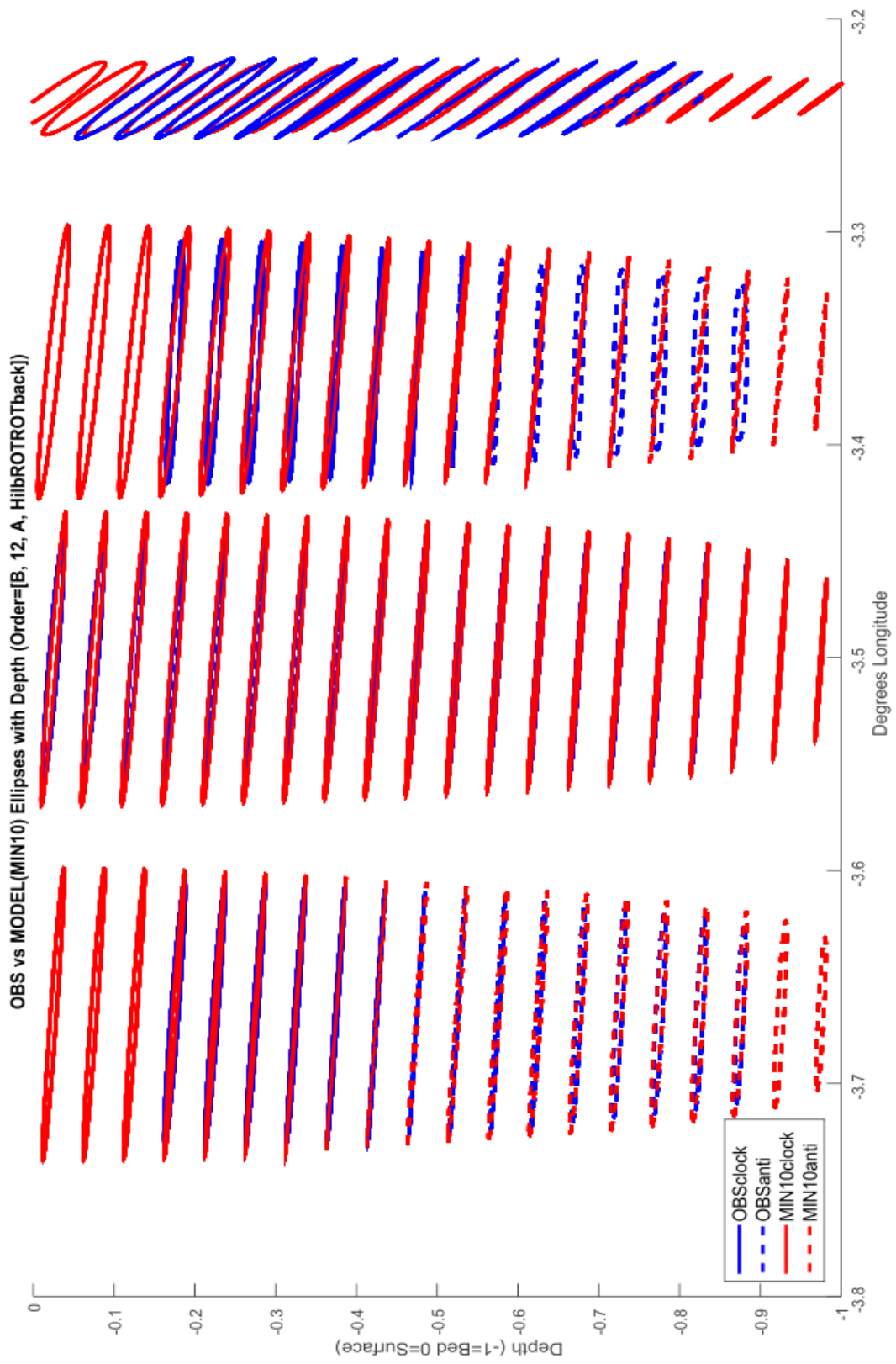


Figure 12: As in Fig. 10, but for the 'MinDepth10' simulation.

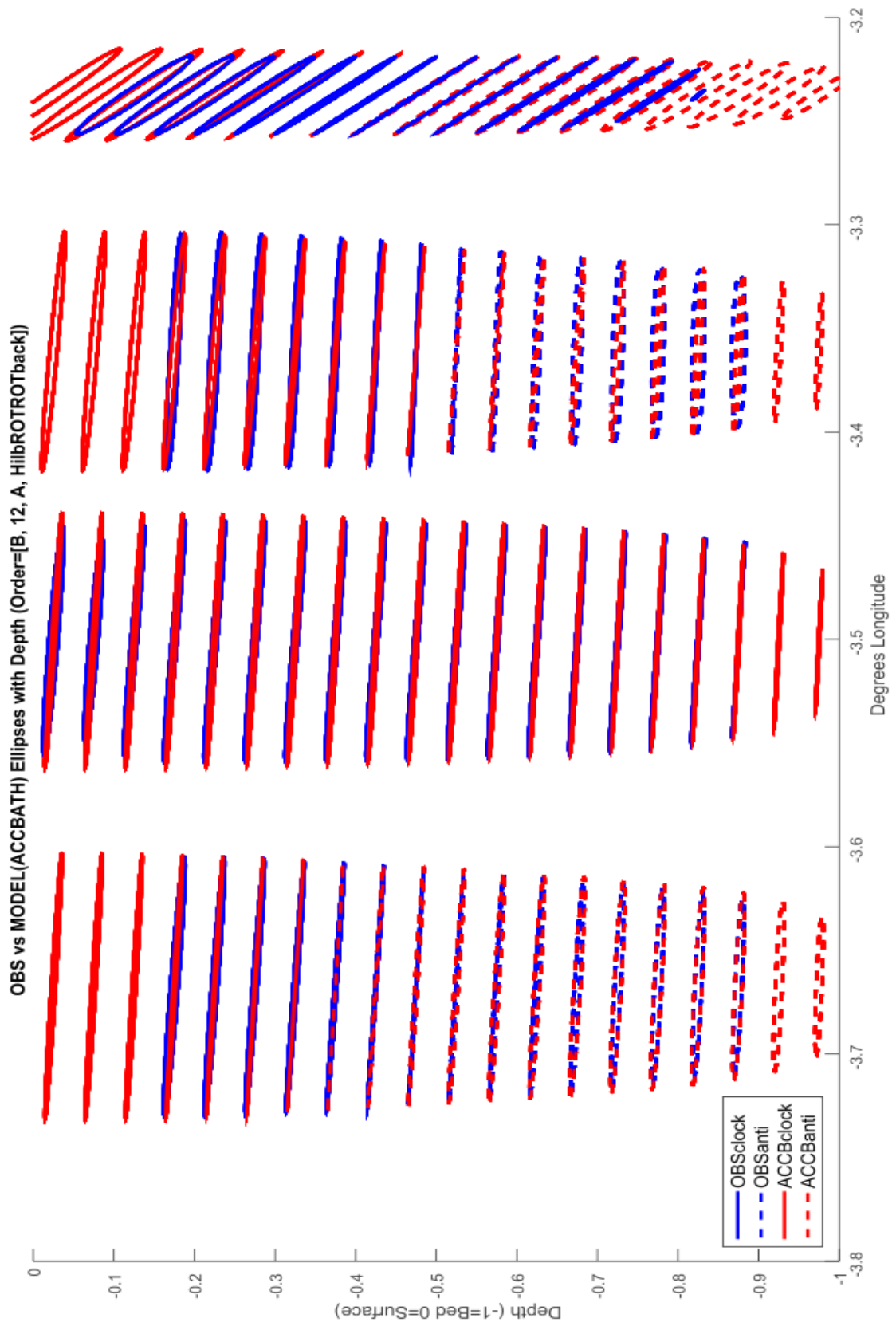


Figure 13: As in Fig. 10, but for the 'AccBath' simulation.

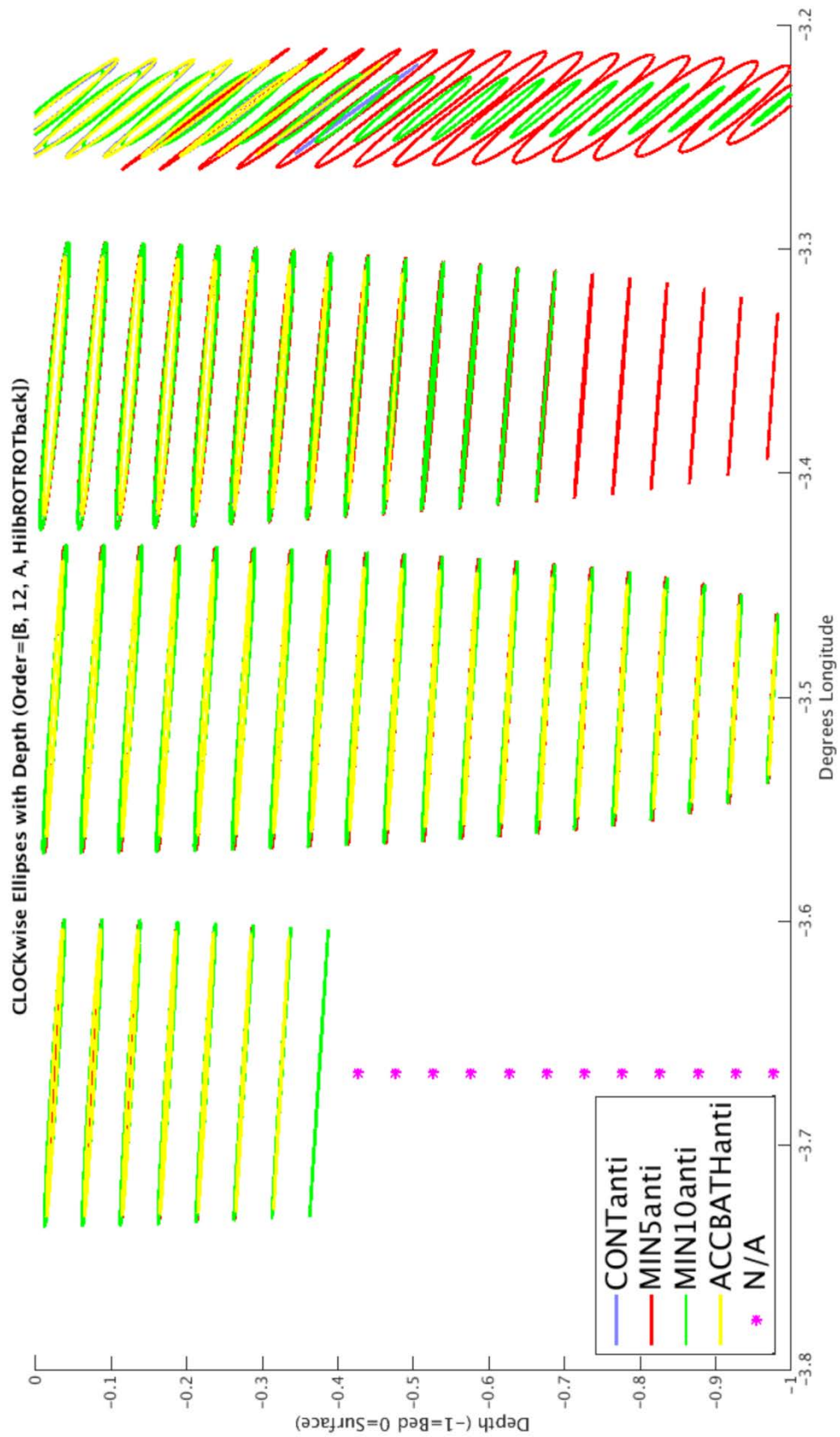


Figure 14: Comparison of the clockwise depth-varying tidal ellipses generated from the 4 model simulations for the 4 sites. NB although the y-axis indicates depth, each ellipse is seen as if it were seen from a bird's eye view (rather than a profile).

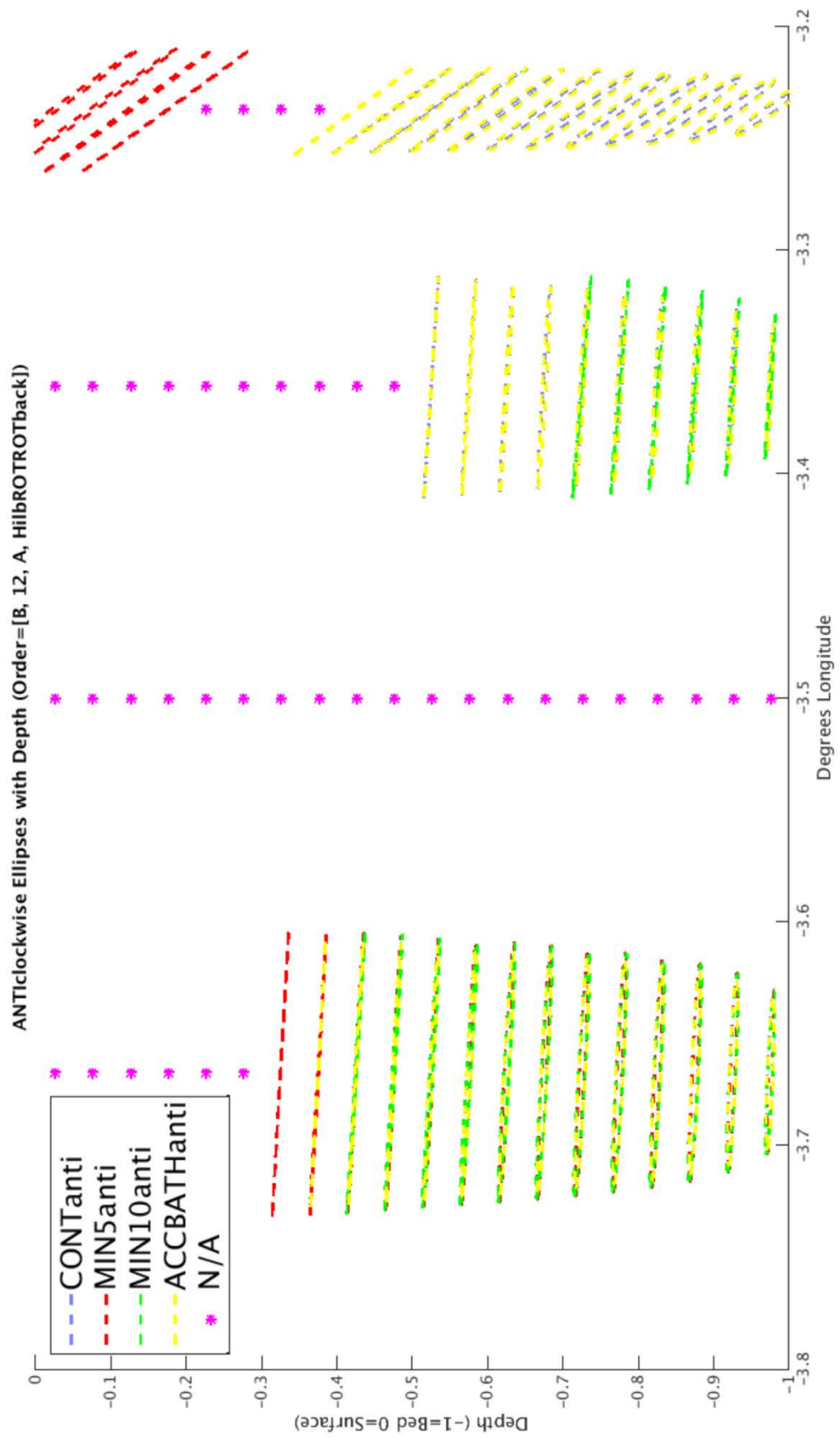


Figure 15: As in Fig. 14, but for the anticlockwise depth-varying tidal ellipses.

3.2. Results: Horizontal-variation in surface ellipses

The following Figures (16-21) show the model performance at the 4 sites. In general the model is found to agree well with the observations. See the error metrics (section 4.2, Tables 13 - 20) for a quantitative comparison between the model derived and observation derived ellipses.

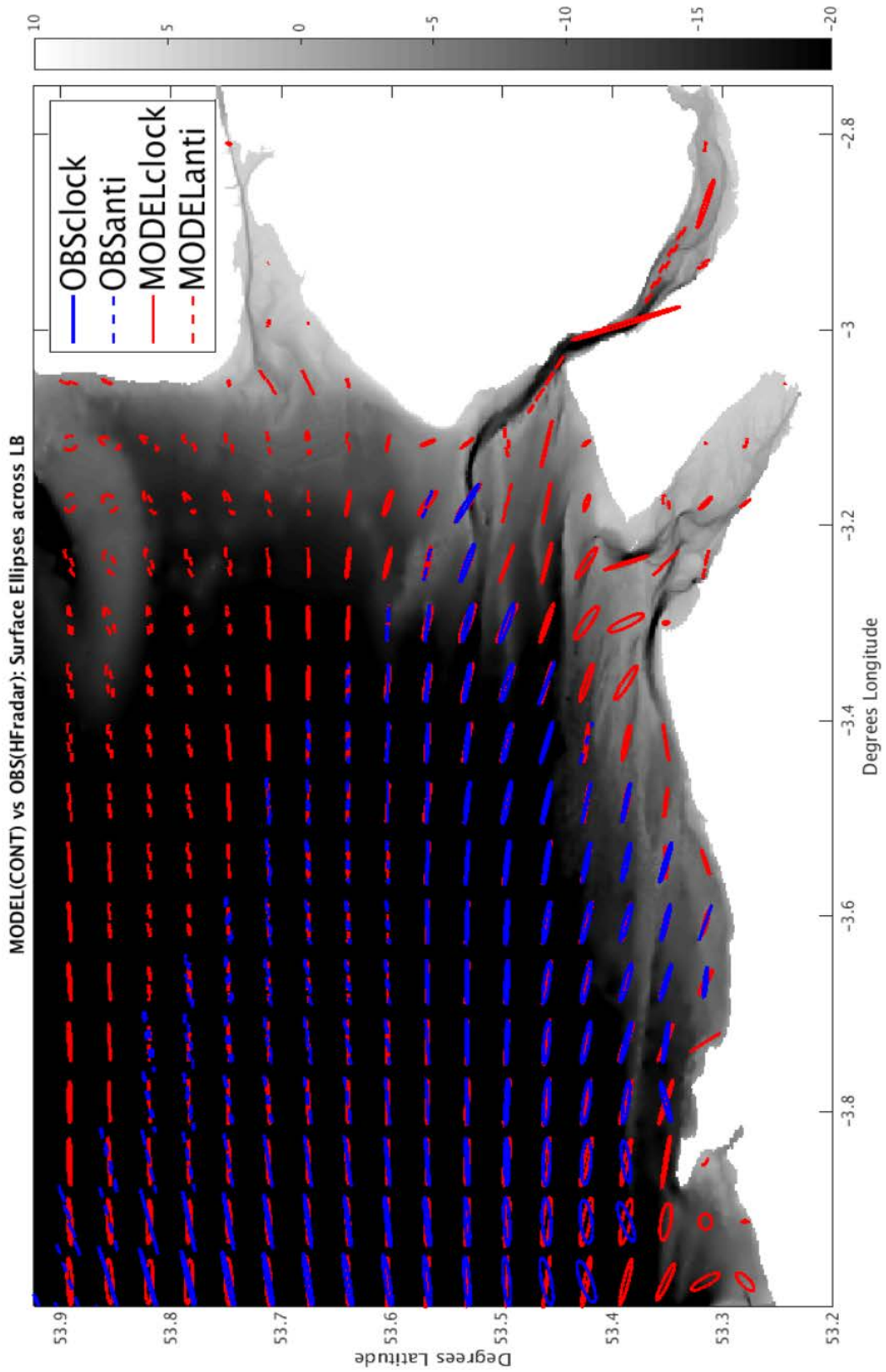


Figure 16: Compares surface tidal ellipses generated from both the HF radar data and the model output for the 'Control' simulation across Liverpool Bay. See Tables 13-20 (Section 4.2) for error metrics relating to surface ellipses.

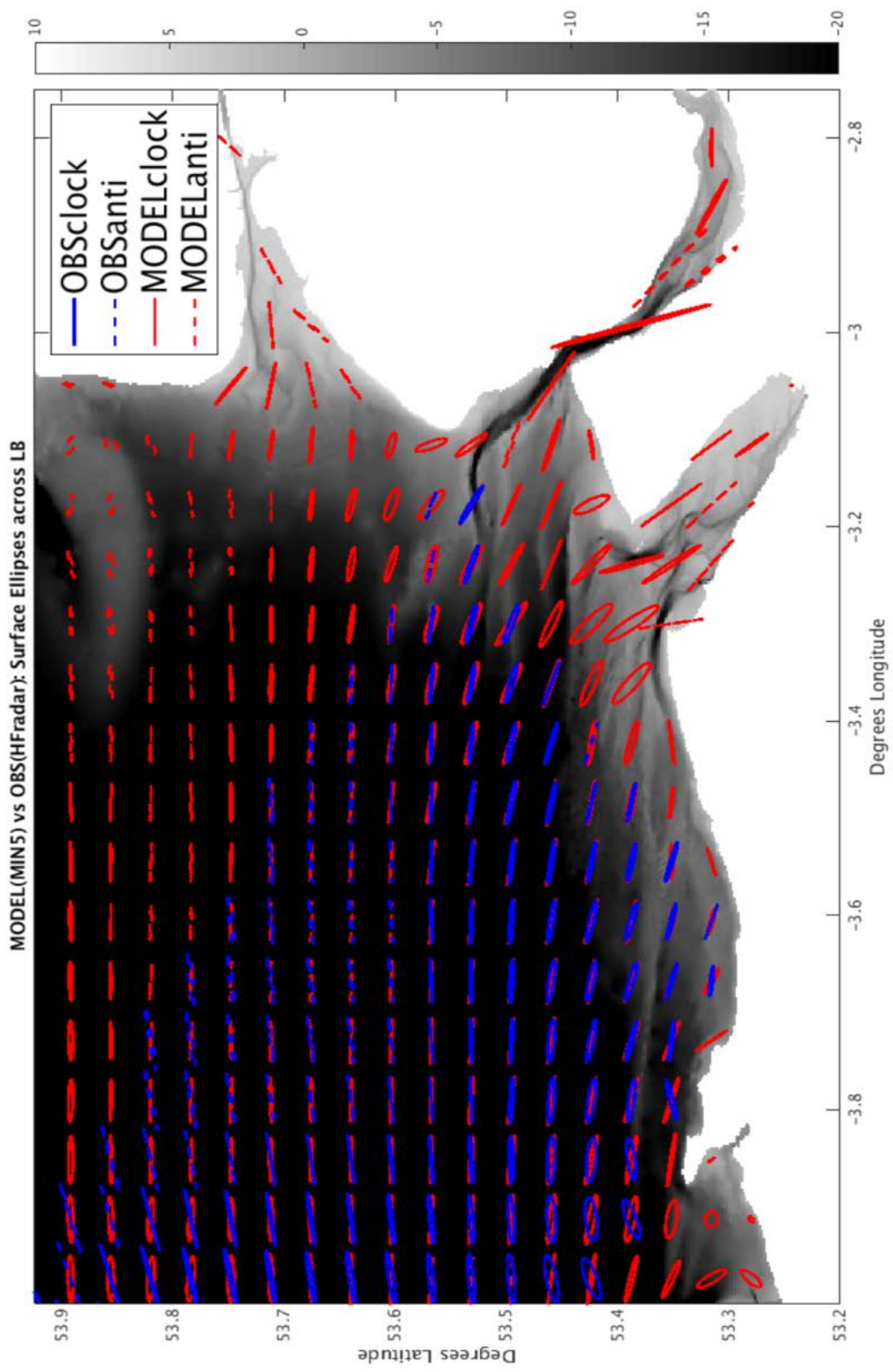


Figure 17: As in Fig. 16, but for the 'MinDepth5' simulation.

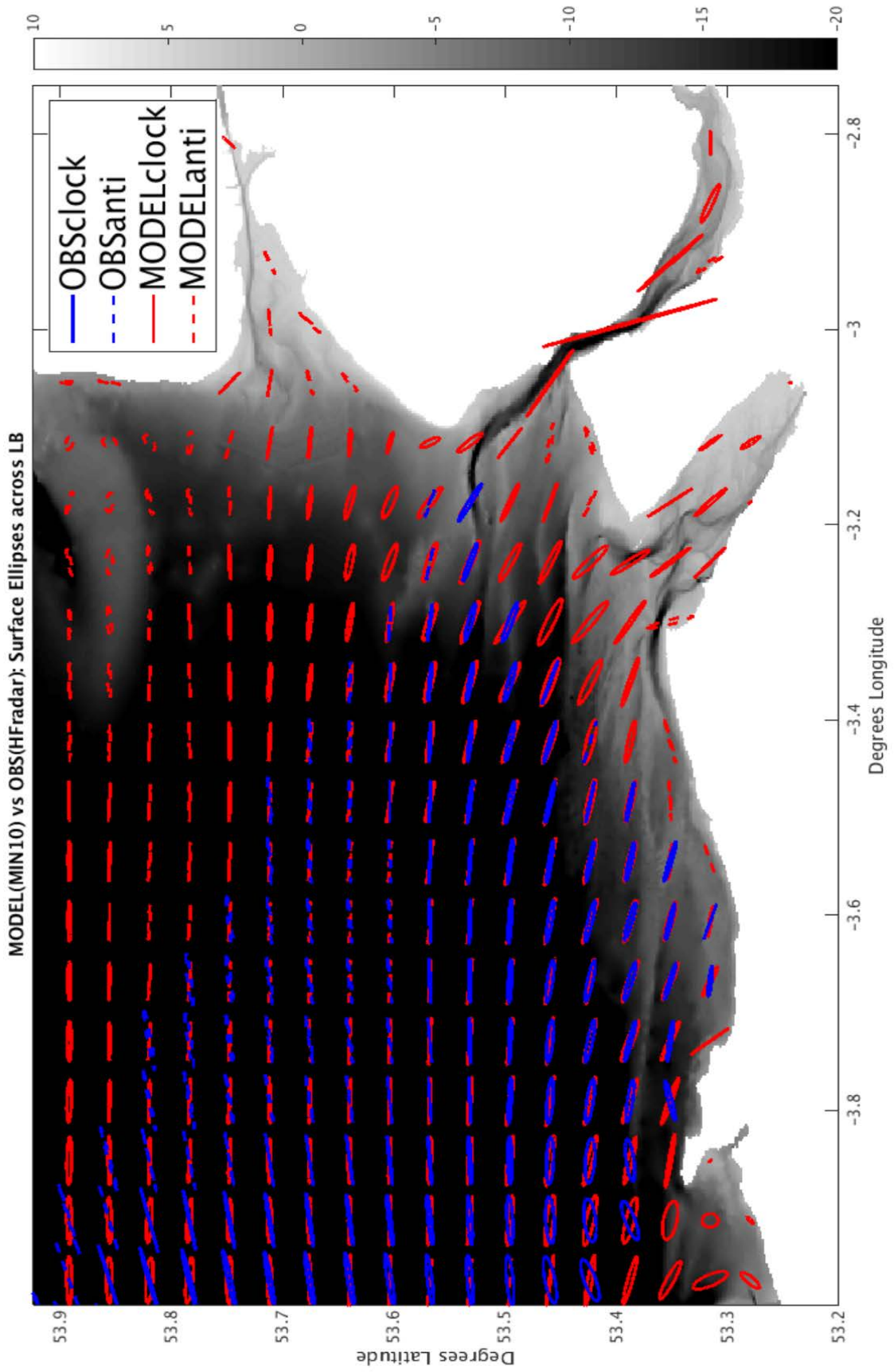


Figure 18: As in Fig. 16, but for the 'MinDepth10' simulation.

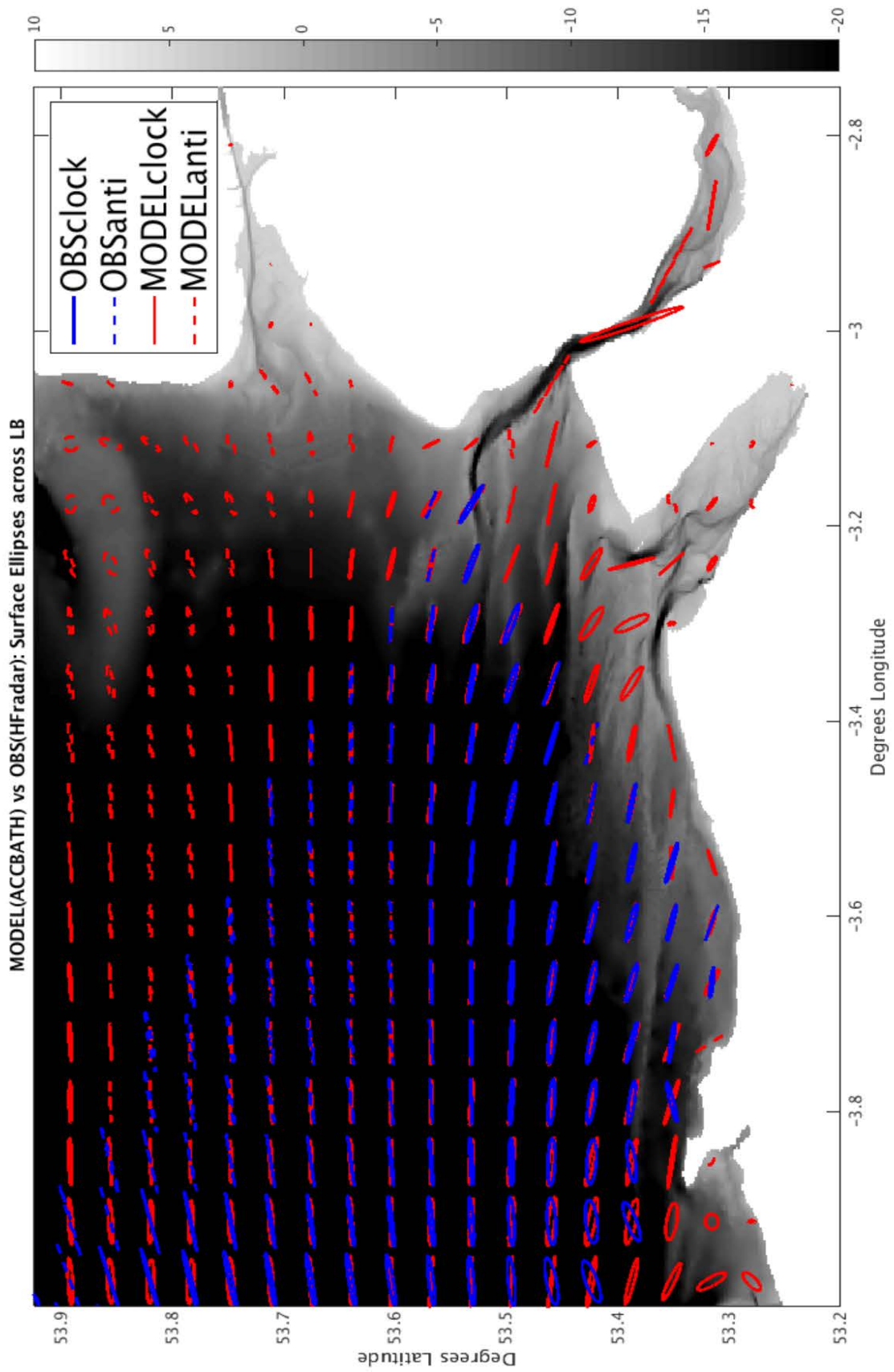


Figure 19: As in Fig. 16, but for the 'AccBath' simulation.

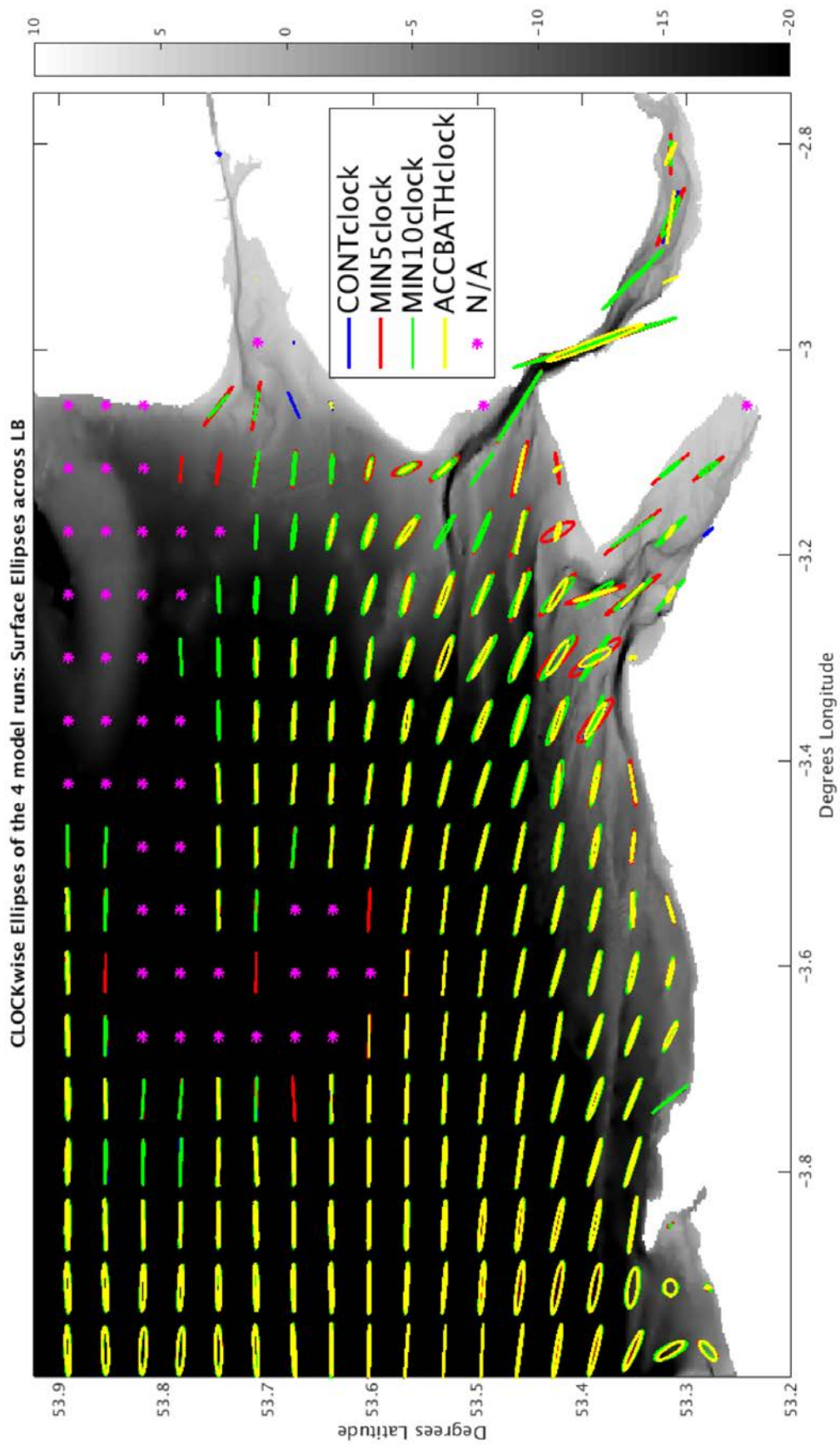


Figure 20: Compares the clockwise surface tidal ellipses generated from the 4 simulations across Liverpool Bay.

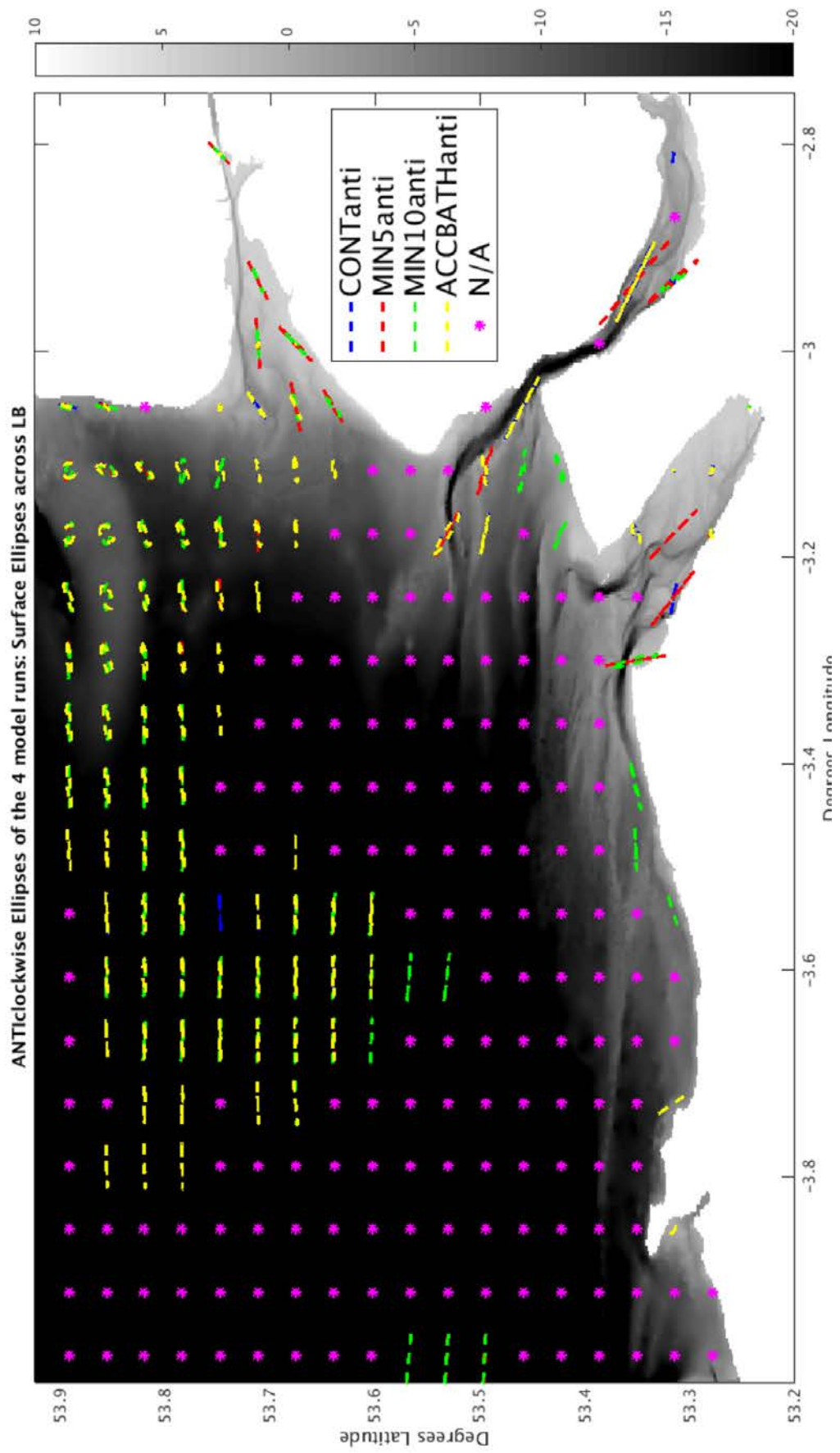


Figure 21: As in Figure Fig. 20, but for the anticlockwise surface tidal ellipses.

3.3. Results: Pre and Post Wind Farm Ellipses

The following Figures (22-23) show the observation derived M_2 ellipses both before (period Dec 07 – Nov 08) and after (period Dec 2010 – Nov 2011) the installation of the RHYL windfarm. Very little difference in the M_2 ellipses can be observed.

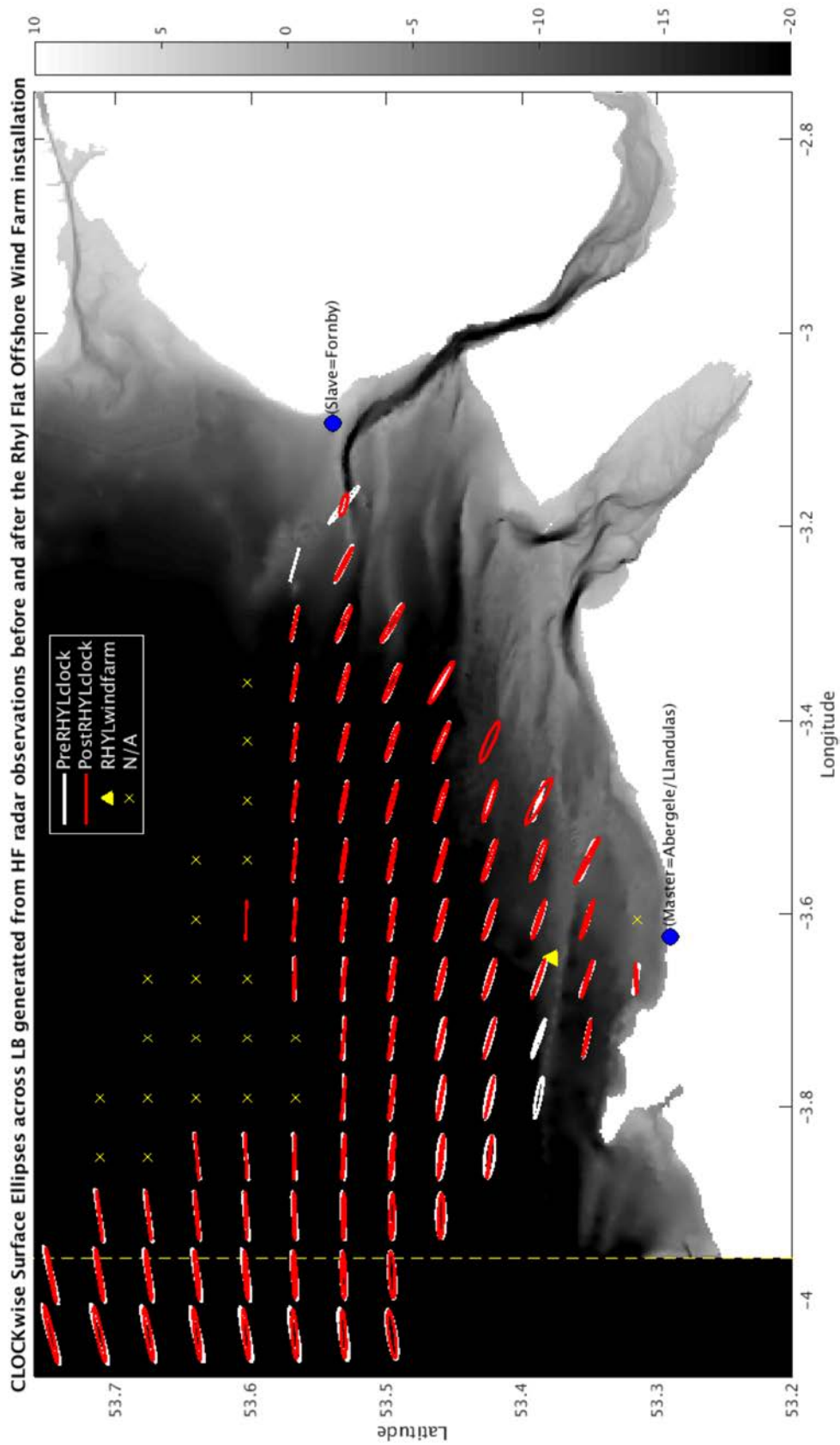


Figure 22: Compares the clockwise surface tidal ellipses generated from the HF radar observations before the installation of the Rhyll Flat Offshore Wind Farm (In white for the period Dec 07 – Nov 08) and after (In red for the period Dec 2010 – Nov 2011) across Liverpool Bay. The dashed yellow line represents where the observed data extends beyond the model domain.

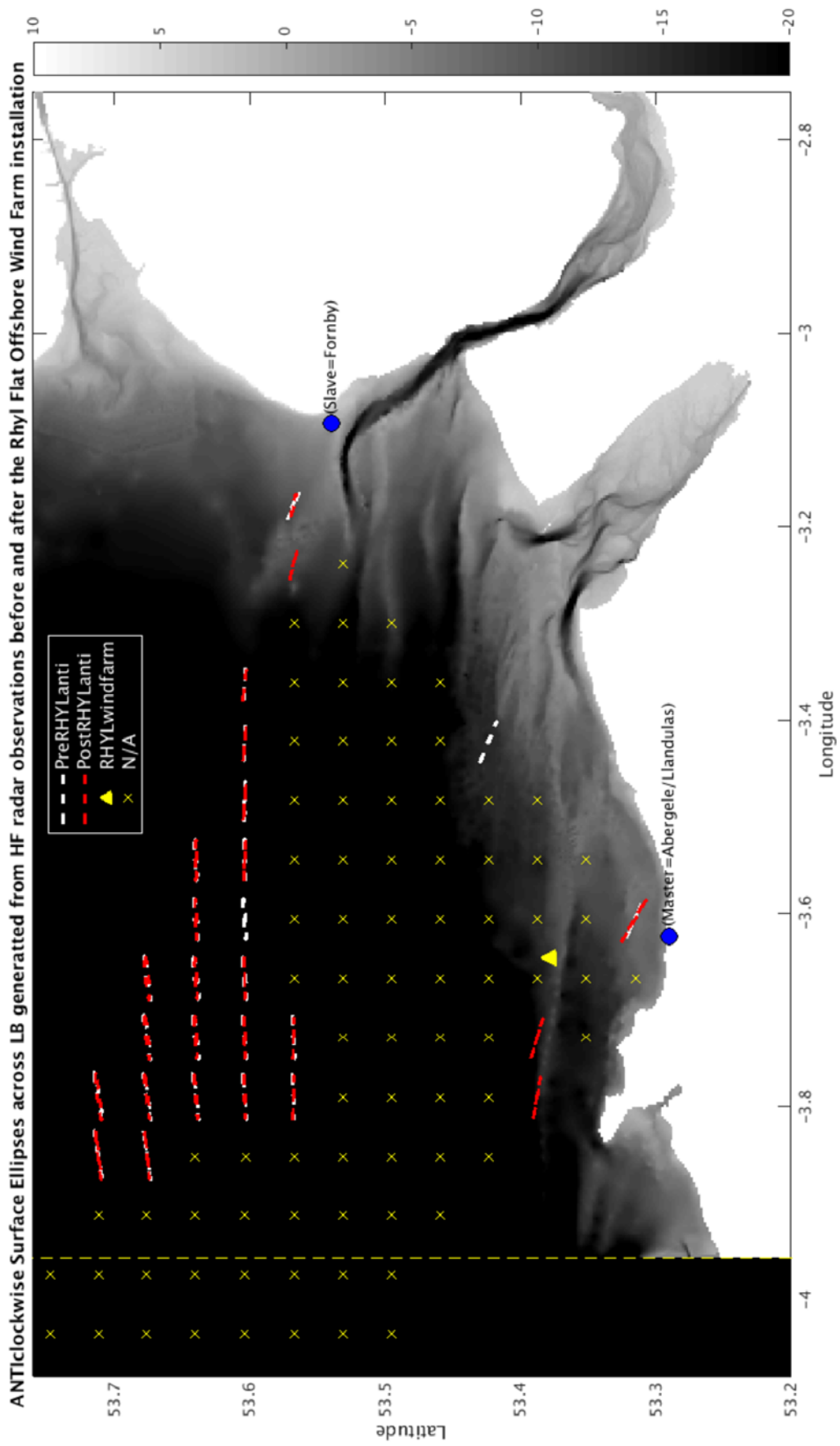


Figure 23: As in Fig. 22, but for the anticlockwise surface tidal ellipses.

4. Results: Error Metrics.

For the following error metrics (Tables 8-23), values highlighted in blue indicate the closest match between observations and model ellipses, while red values indicate the biggest difference.

The following metrics tables are often composed of four parts. The first part shows the value of the error metric in question while the second part expresses these values as an index in order to facilitate easy comparison between the models simulations. The index always takes the closest simulation to the observations as the base (i.e. =100)

e.g. to calculate the RMSE Index for the major axis of Site A (See Table 4) divide each of the 4 values (1 per model simulation) by the minimum of the those 4 values and multiply by 100. As the AccBath simulation is the smallest value its index becomes the base (i.e. 100). The MinDepth5 simulation has a value of 998.14, which means that its RMS error is roughly 10 times bigger than for the AccBath simulation.

Parts 3 and 4 are summary values. The 'Mean of Index' tables takes an average across the 4 indexed parameters and the 'Index of Mean' divides the 4 values of the 'Mean of Index' by the minimum of these values multiplied by 100. While this last step is not always necessary it is useful when none of the four 'Index of the Mean' values is equal to 100. In such instances the 'Index of Mean' re-expresses 'Mean of Index' as an index with the best model simulation equal to 100.

4.1. Depth-varying ellipses

Tables 4-12 show the 3 error metrics defined in section 1.4 (depth-averaged) applied to the 4 parameters across the 4 model simulations for the depth-varying ellipses.

Tables 4-8 show the depth-averaged *RMSE* for the depth ellipses. Tables 4-7 show the *RMSE* for Site A, B, H and 12 and Table 8 shows the average *RMSE* across all sites (i.e. [Site A +Site B +Site H +Site 12]/4)

Tables 9-10 show the depth-averaged *Bias* for the depth ellipses. Table 9 shows the *Bias* across each of the 4 sites and Table 10 averages the *Bias* across all 4 sites.

Tables 11-12 show the depth-averaged *Model Skill (D)* for the depth ellipses. Table 11 shows the *D* across each of the 4 sites and Table 12 averages the *D* across all 4 sites.

Table 4: ADCP vs Model runs *RMSE* for site A depth-averaged ellipses.

	Control	MinDepth5	MinDepth10	AccBath
Major Axis (m/s)	0.0008	0.0073	0.0070	0.0007
Minor Axis (m/s)	0.0027	0.0040	0.0038	0.0026
Orientation (degrees)	4.94	7.87	8.40	4.74
Rotational Direction	0.00	0.73	0.52	0.00

Index of RMSE				
Major Axis	110.14	998.14	961.14	100.00
Minor Axis	104.00	151.90	146.90	100.00
Orientation (degrees)	104.16	165.80	177.10	100.00
Rotational Direction	Perfect	N/A	N/A	Perfect
Mean of Index	106.10	438.61	428.38	100.00
Index of Mean	106.10	438.61	428.38	100.00

Table 5: ADCP vs Model runs RMSE for site B depth-averaged ellipses.

	Control	MinDepth5	MinDepth10	AccBath
Major Axis (m/s)	0.0018	0.0050	0.0053	0.0016
Minor Axis (m/s)	0.0008	0.0030	0.0025	0.0006
Orientation (degrees)	0.96	0.87	1.63	1.01
Rotational Direction	0.45	0.52	0.37	0.45
Index of RMSE				
Major Axis	112.69	310.74	330.05	100.00
Minor Axis	128.12	467.99	393.03	100.00
Orientation	110.12	100.00	187.86	116.32
Rotational Direction	122.47	141.42	100.00	122.47
Mean of Index	118.35	255.04	252.73	109.70
Index of Mean	107.89	232.49	230.39	100.00

Table 6: ADCP vs Model runs RMSE for site Hilbre depth-averaged ellipses.

	Control	MinDepth5	MinDepth10	AccBath
Major Axis (m/s)	0.0175	0.0383	0.0209	0.0174
Minor Axis (m/s)	0.0012	0.0029	0.0021	0.0013
Orientation (degrees)	0.91	0.73	1.41	0.74
Rotational Direction	0.89	0.73	0.82	0.86
Index of RMSE				
Major Axis	100.81	220.50	120.60	100.00
Minor Axis	100.00	244.40	175.82	107.69
Orientation	124.44	100.00	192.14	100.48
Rotational Direction	122.47	100.00	111.80	117.26

Mean of Index	111.93	166.22	150.09	106.36
----------------------	--------	--------	--------	--------

Index of Mean	105.24	156.29	141.12	100.00
----------------------	--------	--------	--------	--------

Table 7: ADCP vs Model runs RMSE for site 12 depth-averaged ellipses.

	Control	MinDepth5	MinDepth10	AccBath
Major Axis (m/s)	0.0038	0.0090	0.0097	0.0036
Minor Axis (m/s)	0.0013	0.0017	0.0014	0.0014
Orientation (degrees)	2.29	1.54	0.67	2.38
Rotational Direction	0.00	0.00	0.00	0.00

Index of RMSE				
Major Axis	106.77	254.81	273.40	100.00
Minor Axis	100.00	135.29	109.07	106.67
Orientation	340.23	228.15	100.00	354.08
Rotational Direction	NaN	NaN	NaN	NaN

Mean of Index	182.33	206.08	160.82	186.92
----------------------	--------	--------	--------	--------

Index of Mean	113.38	128.14	100.00	116.22
----------------------	--------	--------	--------	--------

Table 8: ADCP vs Model runs RMSE averaged over all sites.

	Control	MinDepth5	MinDepth10	AccBath
Major Axis (m/s)	0.0060	0.0149	0.0107	0.0058
Minor Axis (m/s)	0.0015	0.0029	0.0024	0.0015
Orientation (degrees)	2.28	2.75	3.03	2.22
Rotational Direction	0.34	0.49	0.42	0.33

Index of RMSE				
Major Axis	102.83	256.43	184.80	100.00
Minor Axis	101.82	196.36	166.62	100.00
Orientation	102.55	123.98	136.52	100.00
Rotational Direction	102.92	151.66	130.26	100.00

Mean of Index	102.53	182.11	154.55	100.00
----------------------	--------	--------	--------	--------

Table 9: ADCP vs Model runs (depth-averaged) *Bias* for the 4 sites.

Site A	Control	MinDepth5	MinDepth10	AccBath
Major Axis (m/s)	0.0004	0.0073	0.0070	-0.0001
Minor Axis (m/s)	-0.0022	-0.0010	-0.0019	-0.0022
Orientation (degrees)	-4.89	-7.79	-8.32	-4.69
Rotational Direction	0.00	0.53	0.27	0.00

Site B	Control	MinDepth5	MinDepth10	AccBath
Major Axis (m/s)	0.0014	0.0048	0.0052	0.0012
Minor Axis (m/s)	-0.0005	0.0007	-0.0001	-0.0005
Orientation (degrees)	0.16	-0.02	-1.28	0.17
Rotational Direction	-0.20	-0.27	-0.13	-0.20

Site H	Control	MinDepth5	MinDepth10	AccBath
Major Axis (m/s)	0.0111	0.0361	-0.0156	0.0108
Minor Axis (m/s)	0.0009	0.0021	0.0013	0.0009
Orientation (degrees)	-0.41	-0.16	1.11	-0.17
Rotational Direction	0.13	0.53	0.67	0.07

Site 12	Control	MinDepth5	MinDepth10	AccBath
Major Axis (m/s)	0.0023	0.0084	0.0090	0.0019
Minor Axis (m/s)	-0.0006	0.0006	-0.0002	-0.0005
Orientation (degrees)	2.26	1.48	-0.50	2.35
Rotational Direction	0.00	0.00	0.00	0.00

Table 10: ADCP vs Model runs *Bias* averaged over all sites.

DE_Bias: ALLSITES	Control	Mindepth5	Mindepth10	AccBath
Major Axis	0.0038	0.0142	0.0014	0.0035
Minor Axis	-0.0006	0.0006	-0.0002	-0.0006
Orientation	-0.72	-1.62	-2.25	-0.58
Rotational Direction	-0.02	0.20	0.20	-0.03

Bias% relative to mean(obs)	Control	MinDepth5	MinDepth10	AccBath
Major axis	6.60	24.70	2.44	6.04
Minor Axis	-21.23	20.76	-8.35	-20.09

Table 11: ADCP vs Model runs (depth-averaged) *Model Skill (D)* for the 4 sites.

Site A	Control	MinDepth5	MinDepth10	AccBath
Major Axis	1.00	0.77	0.79	1.00
Minor Axis	0.66	0.24	0.38	0.68
Orientation	0.45	0.31	0.29	0.46
Rotational Direction	1.00	0.50	0.74	1.00

Site B	Control	MinDepth5	MinDepth10	AccBath
Major Axis	0.98	0.85	0.85	0.98
Minor Axis	0.90	0.31	0.40	0.94
Orientation	0.75	0.81	0.60	0.71
Rotational Direction	0.79	0.72	0.86	0.79

Site H	Control	MinDepth5	MinDepth10	AccBath
Major Axis	0.50	0.36	0.57	0.51
Minor Axis	0.72	0.44	0.57	0.67
Orientation	0.39	0.21	0.33	0.40
Rotational Direction	0.10	0.55	0.47	0.14

Site 12	Control	MinDepth5	MinDepth10	AccBath
Major Axis	0.80	0.48	0.46	0.82
Minor Axis	0.41	0.63	0.72	0.32
Orientation	0.45	0.56	0.76	0.44
Rotational Direction	NaN	NaN	NaN	NaN

Table 12: ADCP vs Model runs *Model Skill (D)* averaged over all sites and the average *Model Skill (D)* over the 4 parameters.

ALLSITES	Control	MinDepth5	MinDepth10	AccBath
Major Axis	0.82	0.62	0.67	0.83
Minor Axis	0.67	0.40	0.49	0.65
Orientation	0.51	0.47	0.55	0.50
Rotational Direction	0.72	0.69	0.73	0.73
Average D over 4 param	0.68	0.55	0.61	0.68

4.2. Error Metrics: Horizontal-variation in surface ellipses.

Tables 13-20 show the 3 error metrics defined in section 1.4 applied to the 4 parameters across the 4 model simulations for the horizontal-variation in surface ellipses.

Tables 13-16 show the *RMSE* for the surface ellipses. Tables 13-15 show the *RMSE* for HF radar cells located within the bathymetry depth range 0-10 m, 10-20 m and 20+ m respectively. Table 15 shows the *RMSE* averaged over all 136 HF radar cells. The combined *RMSE* is plotted in Figure 24 to visualise the spatial variability in the model error.

Table 17-18 show the averaged *Bias* for the surface ellipses. Table 17 shows the *Bias* across each of the 3 bathymetry depth ranges and Table 18 shows the *Bias* averaged over all 136 HF radar cells.

Table 19-20 show the averaged *Model Skill (D)* for the surface ellipses. Table 19 shows the *D* across each of the 3 bathymetry depth ranges and Table 20 shows the *D* averaged over all 136 HF radar cells.

Table 13: HF radar vs Model runs *RMSE* for the 3 surface ellipse cell locations with a bathymetry of between 0-10m

0-10 m	Control	MinDepth5	MinDepth10	AccBath
Major Axis (m/s)	0.1044	0.0889	0.0783	0.1039
Minor Axis (m/s)	0.0325	0.0353	0.0193	0.0329
Orientation (degrees)	11.71	11.46	11.42	11.74
Rotational Direction	6.81	6.81	6.78	6.81

Index of RMSE				
Major Axis	133.36	113.53	100.00	132.77
Minor Axis	168.58	183.33	100.00	170.66
Orientation	102.57	100.42	100.00	102.86
Rotational Direction	100.36	100.36	100.00	100.36

Mean of Index				
	126.22	124.41	100.00	126.66

Index of Mean				
	126.22	124.41	100.00	126.66

Table 14: HF radar vs Model runs *RMSE* for the 20 surface ellipse cell locations with a bathymetry of between 10-20m

10-20 m	Control	MinDepth5	MinDepth10	AccBath
Major Axis (m/s)	0.0490	0.0623	0.0752	0.0509
Minor Axis (m/s)	0.0209	0.0423	0.0423	0.0184
Orientation (degrees)	9.69	10.23	10.31	9.66
Rotational Direction	2.58	2.58	2.58	2.58

Index of <i>RMSE</i>				
Major Axis	100.00	127.13	153.50	103.89
Minor Axis	113.81	230.33	230.46	100.00
Orientation	100.38	105.93	106.73	100.00
Rotational Direction	100.00	100.00	100.00	100.00

Mean of Index	103.55	140.85	147.67	100.97
----------------------	--------	--------	---------------	---------------

Index of Mean	102.55	139.49	146.25	100.00
----------------------	--------	--------	---------------	---------------

Table 15: HF radar vs Model runs *RMSE* for the 113 surface ellipse cell locations with a bathymetry of between 10-20m.

20 m+	Control	MinDepth5	MinDepth10	AccBath
Major Axis (m/s)	0.1441	0.1345	0.1334	0.1449
Minor Axis (m/s)	0.0331	0.0382	0.0352	0.0325
Orientation (degrees)	7.60	8.77	9.41	7.54
Rotational Direction	0.63	0.70	0.68	0.61

Index of <i>RMSE</i>				
Major Axis	108.00	100.78	100.00	108.57
Minor Axis	101.72	117.34	108.23	100.00
Orientation	100.80	116.30	124.82	100.00
Rotational Direction	103.35	114.81	111.80	100.00

Mean of Index	103.47	112.31	111.21	102.14
----------------------	--------	---------------	--------	---------------

Index of Mean	101.30	109.95	108.88	100.00
----------------------	--------	---------------	--------	---------------

Table 16: HF radar vs Model runs *RMSE* for the all 136 surface ellipse cell locations.

All Depths	Control	MinDepth5	MinDepth10	AccBath
Major Axis	0.1345	0.1263	0.1262	0.1352
Minor Axis	0.0317	0.0387	0.0360	0.0310
Orientation (degrees)	8.02	9.04	9.58	7.97
Rotational Direction	0.46	0.54	0.51	0.44

Index of <i>RMSE</i>				
Major Axis	106.58	100.11	100.00	107.20
Minor Axis	102.25	124.78	116.07	100.00
Orientation	100.67	113.51	120.28	100.00
Rotational Direction	105.41	123.23	117.06	100.00

Mean of Index				
	103.73	115.41	113.35	101.80

Index of Mean				
	101.89	113.37	111.35	100.00

Table 17: HF radar vs Model runs *Bias* for the 3 surface ellipse depth ranges.

0-10 m	Control	MinDepth5	MinDepth10	AccBath
Major Axis (m/s)	-0.0637	-0.0481	-0.0568	-0.0709
Minor Axis (m/s)	0.0309	0.0117	0.0162	0.0314
Orientation (degrees)	-5.72	-4.25	-3.51	-5.89
Rotational Direction	-0.33	-0.33	0.00	-0.33

10-20 m	Control	MinDepth5	MinDepth10	AccBath
Major Axis (m/s)	-0.0234	0.0310	0.0530	-0.0269
Minor Axis (m/s)	0.0026	0.0166	0.0314	0.0008
Orientation (degrees)	-2.86	-3.93	-6.08	-2.78
Rotational Direction	0.25	0.25	0.25	0.25

20 m+	Control	MinDepth5	MinDepth10	AccBath
Major Axis (m/s)	-0.2185	-0.1328	-0.1558	-0.2232
Minor Axis (m/s)	-0.0068	-0.0071	-0.0042	-0.0069
Orientation (degrees)	-5.94	-7.52	-8.23	-5.84
Rotational Direction	0.18	0.22	0.21	0.16

Table 18: HF radar vs Model runs *Bias* for all 136 surface ellipse cell locations.

All Depths	Control	MinDepth5	MinDepth10	AccBath
Maj	-0.0779	-0.0469	-0.0376	-0.0799
Min	-0.0050	-0.0033	0.0026	-0.0055
Theta	-5.52	-6.97	-7.84	-5.43
RD	0.20	0.22	0.19	0.18

Bias% relative to mean(obs)				
Maj	-10.99	-6.61	-5.30	-11.28
Min	-13.00	-8.56	6.78	-14.25

Table 19: HF radar vs Model runs *Model Skill (D)* for the 3 surface ellipse depth ranges.

0-10 m	Control	MinDepth5	MinDepth10	AccBath
Major Axis	0.78	0.82	0.64	0.77
Minor Axis	0.62	0.21	0.74	0.63
Orientation	0.58	0.50	0.60	0.58
Rotational Direction	0.00	0.00	NaN	0.00

10-20 m	Control	MinDepth5	MinDepth10	AccBath
Major Axis	0.80	0.65	0.55	0.79
Minor Axis	0.62	0.24	0.38	0.70
Orientation	0.47	0.47	0.48	0.47
Rotational Direction	0.43	0.43	0.43	0.43

20 m+	Control	MinDepth5	MinDepth10	AccBath
Major Axis	0.65	0.61	0.59	0.65
Minor Axis	0.65	0.54	0.62	0.66
Orientation	0.73	0.70	0.67	0.73
Rotational Direction	0.69	0.63	0.63	0.71

Table 20: HF radar vs Model runs *Model Skill (D)* for the all 136 surface ellipse cell locations and the average *Model Skill (D)* over the 4 parameters.

All Depths	Control	MinDepth5	MinDepth10	AccBath
Major Axis	0.59	0.55	0.52	0.60
Minor Axis	0.62	0.47	0.58	0.64
Orientation	0.78	0.75	0.74	0.78
Rotational Direction	0.71	0.59	0.64	0.74

Average D over 4 param				
	0.68	0.59	0.62	0.69

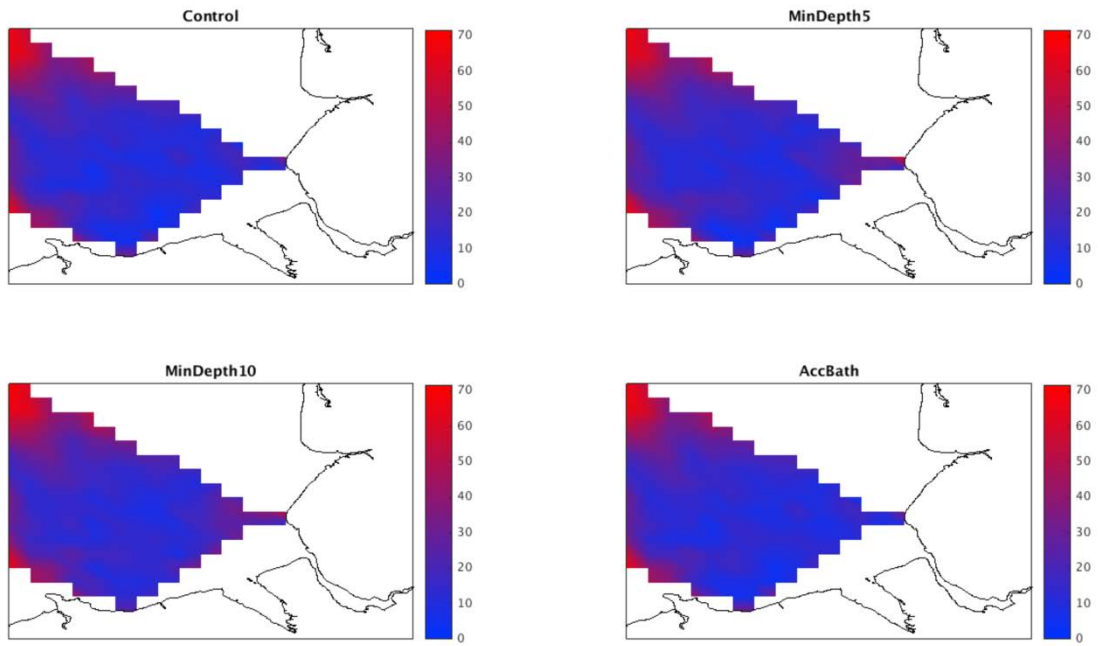


Figure 24: Shows the combined RMSE (See section 2.4.3) across Liverpool Bay for each model simulation. A combined RMSE error of '0' indicates no combined RMSE error. Higher values (up to a possible maximum of 100) indicate a higher combined RMSE error. A value of '100' would indicate that an individual model ellipse had the greatest RMSE (across the bay) for its major axis, minor axis and orientation simultaneously.

5. Results summary: Depth-varying ellipses

- For sites A, B and H the *RMSE* across all 4 parameters is lowest for the AccBath simulation (See tables 4-6) followed closely by the Control simulation. MinDepth5 and MinDepth10 have a higher *RMSE*.
- Site 12 is an exception to this pattern as the MinDepth10 has the lowest *RMSE* across all 4 parameters followed by the Control and AccBath simulations followed by MinDepth5 with the highest *RMSE* (See Table 7)
- When averaged across all 4 sites the AccBath and Control simulations have the lowest *RMSE* index across all 4 parameters (100 and 103 respectively; See Table 8) compared with MinDepth10 and MinDepth5 (155 and 182 respectively; See Table 8).
- The model tends to over predict the major axis of the depth ellipses (ranging from +2 to +25%) depending on the simulation. MinDepth5 has the greatest over-prediction but this is mainly due to error in the simulation at the Hilbre Site, as well as Site A but to a lesser extent.
- The model tends to under-predict the minor axis (ranging from -21% to 21%; See Table 10) with the MinDepth5 simulation over predicting (+21%) on average mainly due to site Hilbre.
- The model appears to predict ellipses which are slightly rotated clockwise relative to the ellipses generated by models (ranging from -0.6 to 2.3 degrees; See Table 10.)
- The model appears to have no particular *Bias* regarding ellipse rotational direction (See Table 10).
- The *Model Skill (D)* averaged across all 4 parameters seems to be greatest for the Control and AccBath simulations (0.68 and 0.68 respectively; See Table 12). This is followed in accuracy by MinDepth10 (0.61) and MinDepth5 (0.55).

5.1. Results summary: Horizontal-variation in surface ellipses

- For the depth range 0-10 m where only 3 HF radar cells are located, the MinDepth10 simulation gives the lowest *RMSE* index when averaged across the 4 parameters. MinDepth5, Control and AccBath simulations give a similar *RMSE* index (See Table 13).
- For the 10-20 m, 20 m+ and all depth ranges combined the AccBath simulation has the lowest *RMSE* index followed closely by the Control simulation. When all depth locations are taken into account the MinDepth5 simulation has the highest *RMSE* index.
- The model simulations in general tend to under-predict the size of the major and minor axes. Ranging from -11% to -5% for the major axis (See Table 18) and Ranging from -14% to -7% for the minor axis. The biases are evident particularly in the west of Liverpool Bay.
- The model appears to predict ellipses which are orientated clockwise relative to the observations (ranging from 5.4 to 7.8 degrees further clockwise; See Table 18). This *Bias* appears to be bigger than the orientation *Bias* for the depth-varying ellipses.
- The model appears to have a slight tendency to over predict the number of clockwise rotating and under predict anticlockwise rotating ellipses (See Table 18).
- The *Model Skill (D)* averaged across all 4 parameters and all HF radar points seems to be greatest for the AccBath and Control simulations (0.69 and 0.68 respectively; See Table 20) followed by MinDepth10 (0.62) and MinDepth5 (0.59). These averaged *Model Skills* are remarkably similar to those for the depth-varying ellipses.

5.2 Discussion: Tidal Ellipses pre and post wind farm.

- Only slight differences are evident in the M_2 ellipses pre and post windfarm installation in the vicinity of the Rhyl wind farm.
- Slight differences also appear to be evident at some distance from the wind farm.
- Any changes that are evident could also be due to other factors such as changes in the bathymetry across the domain over the 3 year period between the times of observation.
- The M_2 represents the dominant tidal flow within the bay. Although little impact of the windfarm is identified on the typically 1.5m/s tidal currents there could be greater impact on the much weaker residual circulation important for residual transport of sediment and other properties.
- Validation of the M_2 tidal ellipses has shown high model accuracy. This model setup would therefore be suitable to investigate the impact of the windfarm providing a higher resolution grid than the radar to investigate the residual and dominant circulation across the bay.

6. Overall Discussion with Conclusions

Both the *Model Skill (D)* and *RMSE* values for both the horizontally-varying surface and depth-varying ellipses indicate that the AccBath and Control simulations are considerably better than the MinDepth5 and the MinDepth10 simulations.

The AccBath bathymetry generally does marginally better than the Control bathymetry but the difference is small. This tie is unsurprising when one considers that neither bathymetry matches the year modelled (2008) or the date of the observations (2006-2008). The fact AccBath is slightly better suggests that the model accuracy is sensitive to a consistent (in time) coastal bathymetry being applied.

Table 21 shows the *RMSE* and the *Model Skill (D)* as an index averaged over the 4 ellipse properties (axes, orientation and rotation) and over the all ellipses considered in both the depth and horizontal-variations.

Table 21: *RMSE* Index and *Model Skill* averaged (and rounded) over the surface and depth ellipses.

	Control	MinDepth5	MinDepth10	AccBath
RMSE Index	102	148	133	100
Model Skill	0.68	0.57	0.62	0.69

The lower *RMSE* index (closer to 100) and a higher *Model Skill* (closer to 1) indicate a better agreement between the simulations and observational data. For detailed results see Figs. 10-23 and Tables 4-20.

These results support the idea that accurate coastal bathymetry is important in modelling studies, improving predictive ability. While the predictive ability is improved generally there are regional differences. For example looking at the surface ellipses for the MinDepth5 and the AccBath simulations, the orientation of the ellipses is improved in the area near to the entrance of the Mersey, but remains quite poor when predicting the phases of the Surface ellipses to the south west of Liverpool Bay. This is possibly due to the offshore boundary conditions propagating errors from the Irish Sea model. All 4 simulations appear to perform poorly across all 4 parameters in the north west of the Liverpool Bay again possibly due to errors in boundary forcings (see Fig. 24).

Table 22: The model skill averaged over all 4 depth-averaged ellipse parameters at each of the sites for each of the model simulations.

	Control	Min5	Min10	AccBath
Site A	0.78	0.45	0.55	0.78
Site B	0.86	0.67	0.68	0.86
Site H	0.43	0.39	0.48	0.43
Site 12	0.55	0.56	0.65	0.53

While the AccBath and Control simulations are in general better than the MinDepth5 and MinDepth10 when looking at the *Model Skill* (see Table 22) for each of the simulations at each of the sites, MinDepth10 gives the best results when predicting the ellipses for site H and site 12 (see Table 22).

Table 23: The *Model Skill (D)* for each ellipses with depth site-averaged across all model simulations.

	Site B	Site 12	Site A	Site H
D	0.77	0.57	0.61	0.43

Also of interest is that POLCOMS is not as adept at predicting the ellipses (or the u and v currents) for all sites equally. Table 23 shows a large difference in the *Model Skill (D)* between site B (better) and site H (worse). This is possibly due to the fact that site H is within an estuary and site B is at some distance from the coast. Site H is therefore more prone to errors introduced by inaccurate bathymetry.

The degree to which the RHYL windfarm impacted the local hydrodynamics was unable to be ascertained from the M_2 ellipses. This does not necessarily mean that no impacts on the hydrodynamics occurred and future studies might wish to look at the changes in the residual current as this is closely linked to net sediment transport.

Returning to the comments made by Prandle *et al.*, (2011) relating to coastal M_2 tidal ellipses (See section 1.3), we find that:

1. While the spatial resolution of the HF radar observation and model simulation is less than used by Prandle *et al.*'s. (2011, see Fig. 18) Figs. 16-19 do show more rapid variation in ellipse orientation and size offshore closer to the coast than offshore.
2. Prandle *et al.*'s. (2011) comment that ellipses close to the shore tend to have their major axes more directed towards the shore. While we may not be able to witness this due to insufficient spatial resolution in both the model and the HF radar observations, no particular ellipse orientation is evident next to the coast (See Figs. 16-19).
3. Prandle *et al.*'s. (2011) comments that surface ellipse rotational direction tends to be biased clockwise while near-bed rotational direction tends to be biased anticlockwise. Both our model and observational results (See Figs. 10-15) appear to confirm this. A large majority of the surface ellipses are rotating clockwise and the near-bed ellipses at 3 of the 4 ADCP sites are rotating anticlockwise. The exception to this is at Site 12 which rotates clockwise throughout the water column. The MinDepth5 simulation for Hilbre predicts anticlockwise rotating ellipses close to the surface but this disagrees with both the ADCP observations and the nearest Mindepth5 surface ellipse.

Acknowledgement

I would like to express my gratitude to Matthew Palmer for advice on how to filter observational data, David McCann for advice on how to plot tidal ellipses, Andrew Lane for explanations relating to the various bathymetries and Alex Souza for the ADCP data.

References

- Amoudry, L. O., 2014. Modelling-based assessment of suspended sediment dynamics in a hypertidal estuary channel. *Ocean Dynamics*. DOI 10.1007/s10236-014-0695-8
- Amoudry, L., Ramirez-Mendoza, R., Souza, A., Brown, J., 2014. Modelling-based assessment of suspended sediment dynamics in a hypertidal estuarine channel. *Ocean Dynamics*. 64(5) 707-722. DOI 10.1007/s10236-014-0695-8.
- BODC website (<http://cobs.pol.ac.uk/wera/>)
- Bolaños, R. and Souza, A., 2010. Measuring hydrodynamics and sediment transport processes in the Dee Estuary, Earth Syst. Sci. Data, **2**, 157-165, doi:10.5194/essd-2-157-2010, 2010.
- Brown, J., Amoudry, L., Souza, A., Rees, J., 2015. Fate and pathways of dredged estuarine sediment spoil in response to variable sediment size and baroclinic coastal circulation. *Journal of Environmental Management*, **149**. 209-221. 10.1016/j.jenvman.2014.10.017.
- Codiga, D.L., 2011. Unified Tidal Analysis and Prediction Using the UTide Matlab Functions. Technical Report 2011-01. Graduate School of Oceanography, University of Rhode Island, Narragansett, RI. 59pp.
<ftp://www.po.gso.uri.edu/pub/downloads/codiga/pubs/2011Codiga-UTide-Report.pdf>
- Holt, J.T., James I. D., 2001. An S coordinate density evolving model for the northwest European continental shelf. Model description and density structure. *Journal of Geophysical Research: Oceans*, **106:C7**, 14015–14034.
- Holt, J.T. 2007. *POLCOMS user guide V6.3*. National Oceanography Centre Liverpool. 43 pp.
- Marsh, T.J. and Sanderson, F.J., 2003. CEH National River Archive: Derivation of daily outflows from Hydrometric Areas.
- Ramirez-Mendoza, R., Souza, A., Amoudry, L., 2014. Modeling flocculation in a hypertidal estuary. *Ocean Dynamics*, **64 (2)**. 301-313. DOI 10.1007/s10236-013-0675-4.
- Robinson, A., 2013. Wind Turbine Impacts on the HF radar ocean surface measurements in Liverpool Bay, Liverpool University PhD Thesis. pp166
- Norman, D., Brown, J.M., Amoudry L.O., Souza A.J., 2014b. Was 2008 a typical year in Liverpool Bay? National Oceanography Centre Internal Document, No. 09, 19pp. 015–14 034.
- Norman, D., Brown, J.M., Amoudry L.O., Souza A.J., 2014a. POLCOMS sensitivity analysis to river temperature proxies, surface salinity flux and river salinity in the Irish Sea. National Oceanography Centre Internal Document, No. 08, 22pp.
- Polton, J.A., Palmer, M.R., Howarth, J.M, 2011. Physical and dynamical oceanography of Liverpool Bay. *Ocean Dynamics*

- Prandle, D., 1982. The vertical structure of tidal currents and other oscillatory flows. *Continental Shelf Research*, 1:2. 191-207.
- Prandle, D., Lane, A. and Souza, A. J., 2011. Coastal Circulation. In: Wolanski, E.; McLusky, D., (eds.) *Treatise on Estuarine and Coastal Science. Volume 2: Water and Fine Sediment Circulation*. Oxford, Elsevier, 237-266.
- Prosser, M. C., Brown, J.M., Plater, A.J., Mills, H., 2015. Comparison of tide-gauge data and a saltmarsh-derived reconstruction of mean sea-level for the Mersey Estuary. National Oceanography Centre Internal Document, No. 14, 44pp.
- Willmott, C.J., 1981. On the Validation of Models. *Physical geography*, **2:2**. 184-194.